

Responses to Referee 1:

We greatly appreciate the valuable comments, and they were very helpful to improve the manuscript. Specific responses are following as per comment.

1. This paper has integrated the logistic regressions with the ecoengineering decision scaling framework to evaluate the risk of system failures in contrast to expected performance under dynamic climate change scenarios. This paper contains new insights and contains a lot of information for scientific community. However, the authors have explained the manuscript in complicated ways which I think could be explained in a simplified manner therefore, the authors are advised to avoid using complex English sentences and try to make their next manuscript as simple as possible which would ultimately increase understanding as well as attract more readers. In a nutshell, the results of this paper are convincing enough to support the basic objective and stance of this paper in its current version. Therefore, after a minor revision, this paper can be given a green signal to be published in journal 'Hydrology and Earth System Sciences (HESS)'.

→ Considering constructive comments from Referee 2, we substantially revised the initial version of our manuscript. The manuscript is now retitled as “incorporating the logistic regression in a decision-centric framework for probabilistic assessment of climate change impacts on a complex water system”. The revised manuscript was focused on the meaning of the logistic regression in decision-centric assessment.

Minor Comments:

1. The authors have used 25 GCMs in current study and all of them have different spatial resolution which has a lot of implications in results section. Therefore the authors are advised to explain how the spatial resolution of all those GCMs are made consistent with each other.

→ They were bias-corrected by a statistical downscaling method. We applied the detrended quantile mapping as described in P6L27-P7L6. By the statistical downscaling, the climate hindcasts and forecasts were bias-corrected towards the observed climates during a reference period. Perhaps, the method is inadequately explained. We will add more explanation there.

2. Page6 Line13: In current study, only high demand scenario has been chosen from a conservative perspective whereas the low demand scenarios has been discarded with the justification of declining rice-planting lands. However the authors did not provide any reference which supports author assumption of declining rice-planting lands.

3. Page6 Line11: Authors are suggested to please explain how they calculated economic growth and effectiveness so that it could be easy for readers to comprehend.

→ Comments 2 and 3 are all related to the demand data, but to improve conciseness of the manuscript, the part that explained the demand projection was removed. This is because this information is available in the given reference (L6-17 in page 6). The revised manuscript is more focused on the logistic surfaces. The decreasing agricultural land is also presented in the given reference

4. Page8 Line27: The line “The four free parameters of GR4J. . .inputs” is confusing and needs to be rephrased. Four free parameters has not been defined yet, therefore, to make it convenient for reader, please first define the four free parameters before abovementioned line.

→ In L8-14 in page 8, GR4J was re-described.

5. Page14 Line14: Please rephrase “more water resources need be transferred” with “more water resources need to be transferred”

→ In revision, the sentence was removed, and replaced with new discussion (from P12L22-P13L4).

6. Page16 Line9: In line “More reliable risk estimates can be achieved from other uncertainty assessment methods though expensive efforts may be required” Please mention few other uncertainty assessment methods you are talking about so that it could be easy for readers to comprehend the context.

→ In revision, we added a part for validation of the logistic regressions using the stochastic sampling (L28 in page 14 and Figure 9).

7. Page24 Figure 1: The annotation color in inset maps needs to be changed because its not clear enough.
→ This might be the resolution problem when converting the word document to a pdf format. We believe that the original figure file would be okay. If necessary, we will make a further improvement.

Responses to Referee 2:

We greatly appreciate valuable efforts of the referee 2. All the comments were sound and constructive to improve our manuscript in the revision process. Specific responses are following as per comment.

General Comments:

This manuscript describes a method of extending a bottom-up climate risk assessment by using logistic regression to estimate the probability that a water system will meet minimum performance criteria over a planning horizon based on the values of climate variables. The method is demonstrated through a case study of water management in the Geum River Basin in South Korea. The Geum River is host to two dams which are managed for water supply, flood control, and environmental flows. The case study analyzes two alternative operating policies' ability to meet both water supply goals and instream flow requirements under a broad range of potential changes in average temperature, average precipitation, and precipitation variability. It is interesting to see the framework applied for multiple sub-basins within a larger system, and important to acknowledge uncertainty that an operating policy will meet a performance goal within specific climate scenarios. The text is poorly written and organized, with many strangely used words that inhibit understanding. Key examples include "successive", "sub-component", and "risk of system failure," which are applied in ways that are not standard in the literature and never clearly defined. Many crucial details related to the methods and motivation do not become clear until carefully examining the results section. For example, I believed the logistic model was simply modeling the water supply/environmental flow reliability as a function of climate variables rather than the risk of falling short of the reliability threshold until carefully examining the figures and results. This was the main point of the manuscript, so it is critically important that it is immediately apparent upon reading the abstract and within every part of the manuscript. The text requires substantial rewording and re-organization to clearly summarize the methodological contribution and motivation earlier in the text, better define scientific notation, and ensure new words and concepts are defined clearly the first time they are introduced. While the goal of the logistic model is a worthy one, it is not clear that the framework has been well executed in the case study or that the novel technical contribution bears sufficient relationship to the EEDS framework to be named for it. This lack of clarity may be a symptom of the confused text. However, based on my understanding of the case study, the methods used to execute the case study are flawed in several important ways. Further, the interpretation of results relies on questionable assumptions related to the fitness of GCM projections for water system risk assessment. Both the manuscript and analysis require major revisions.

→ We substantially revised the manuscript to present the main point from the case study. The revised manuscript retitled as "Incorporating the logistic regression into a decision-centric framework for probabilistic assessment of climate change impacts on a complex water system". This may be better than using the term "logistic EEDS". The revised manuscript focuses on assessing the probabilities of system failures (i.e. system performances less than pre-defined thresholds) using the logistic regressions. The varying performances across the river basin is now not a major part of this work. The terms "successive" and "sub-components" were not used in the revision, while the risk of system failures was still in use. We believe it can be viewed as the probability of unsatisfactory performances against the threshold. Now, the EEDS framework is a case study for an application of the proposed approach. To improve the manuscript, we revised the introduction to emphasize the uncertainty associated with the response surfaces of performance metrics with several prior studies. This implies that risks of unsatisfactory performances can exist even within the climate zone of satisfactory performance in the response surfaces. Incorporating the logistic regression may be an approximate approach to supplement this weakness of the response surfaces. For validating the logistic regressions, we conducted stochastic analysis using the same system models but with arbitrary climate perturbations that were not included in the logistic regressions (Figure 9). The probabilities of satisfactory performances from the stochastic samplings and the logistic model approximately agreed. This will improve the validity of the proposed approach.

The contribution of our work is to combine the logistic regression with the bottom-up approach (not limited to the EEDS) so that users can efficiently quantify the probability of system failures. The value of the logistic regression is to enable to estimate the probability without a large number of realizations. If one estimate it using many (or long) stochastic generations, computational costs would be expensive. When 100 random samplings are applied for a single climatic perturbation, computational costs increase by 100 times. The logistic regression can help to solve this problem. Although it is an approximate approach, the internal variation of 20-year-long stochastic weathers is different from one perturbation to another used in the stress tests. Thus, the impacts of internal climate variation

would be captured in a collective manner by the logistic regression. In revision, we used 539 perturbations for the stress tests with a shorter interval for the mean precipitation. It will reduce the concern that the referee commented.

Specific Comments:

Logistic regression model: (1) Limited calibration set: It is my understanding that the logistic model was calibrated from 434 binary values that correspond to either water supply reliability or environmental flow reliability meeting a threshold under 434 unique combinations of three climate variables. If my understanding is correct, this would mean that there is one response (binary performance metric) per climate scenario (this should be clarified in the manuscript if that is incorrect). This is a very limited data set for analyzing risk of failure resulting from internal climate variability, especially given that each scenario-specific stochastic trace was (a) only 20 years long, and (b) initially identical to every other weather sequence in the analysis that had then been perturbed from the original trace to match a unique combination of average precipitation, average temperature, and precipitation coefficient of variation using quantile mapping. To characterize the effects of internal variability on risk of failure over a planning period, it would be preferable to use the binary reliability outcomes from many more stochastic realizations of weather sequences within each combination of climate variables. With a single stochastic trace perturbed into many climate scenarios, the modelled risk of failure is likely to be driven entirely by the climate scenario rather than the actual risk of missing a performance target under internal climate variability, and furthermore heavily biased across the climate response function by the single stochastic realization used to generate all climate scenarios. This seems to be the opposite of the intentions described in the introduction.

→ As replied to the general comment, we added a validation of the logistic model by testing 100 weather generations for three arbitrarily chosen perturbations that were not used for logistic model. Figure 9 shows that the probability estimates from the logistic model and the stochastic sampling approximately agreed. We believe this would improve validity of the logistic surfaces. Even though one set of weather series was generated for a single climate perturbation, 539 perturbations should have different internal variability due to randomness. Thus, the logistic regression can capture the impact of internal climatic variability in a collective manner.

(2) I do not see any part of the manuscript that assesses the performance of the logistic regression model using out-of-sample data. This is critical to the manuscript's success because it would provide evidence that the loss of information from modelling the risk of failing a satisficing criterion rather than evaluating the risk of failure through many simulations at each combination of climate variables could be worth the savings in computation time.

→ All the logistic regressions applied to the case study are summarized in Table A2 with the McFadden R2. As replied to comment 1, 3 sets of out of sample data were used for validation.

(3) It is not clear whether there are separate logistic regression models for each subbasin, performance metric, etc. How many logistic regression models are there in this case study? One per sub-basin, to model simultaneously meeting water supply reliability and environmental flow requirements? Two per sub-basin, each modelling risk of failing one of the objectives' minimum performance criterion? One, with subbasins represented through dummy variables? If the model is used to predict risk of failing mutual satisficing rather than risk of failing one performance threshold, would the model structure work if the two objectives were in tension (as in the Poff et al. 2015 case study) rather than aligned (as they are in this case study)? This section needs to clearly list the explanatory variables and document the dependent variables much more clearly.

→ All the logistic regressions applied to the case study are presented in Table A2. This will prevent the confusion.

Water system modelling framework:

(1) Synthetic weather generator and streamflow temporal resolution: A daily weather generator is used to generate perturbed weather sequences and run them through a runoff model to generate streamflow. After simulating climate-changed streamflow using the runoff model, daily streamflows are aggregated to monthly flow. Why aggregate ex post rather than using a computationally cheaper weather generator and/or runoff model that is designed to operate at the monthly temporal resolution?

→ This was because validity of the hydrological model. We needed a method for ungauged basins for each sub-basin, and already had a validated model. GR4J was validated by the LOOCV across South Korea by Kim et al. (2017). Though it is true that a monthly model is computationally efficient than daily models, another validation for ungauged basins will be required. Aggregating daily simulations was not very time-consuming, but the main

computational cost in this work was the time required for 20-year-long sequential optimizations. We did not change the model for revision.

(2) Temporal aggregation and precipitation coefficient of variation (cv): Perhaps the monthly streamflow resolution is the reason precipitation coefficient of variation was not a strong predictor of performance metrics? The authors should consider this possibility and potentially discard precipitation cv from their analysis, which might be better served by more stochastic realizations in each climate scenario rather than more climate variables.

→ It is unlikely. Even with the temporal aggregation from daily to monthly values, the monthly flows were affected by P_{cv} . A higher P_{cv} resulted in larger streamflow, because precipitated water would reside in the soil for a shorter length due to more frequent high-intensity rainfall events, leading to less evapotranspiration. We found that P_{cv} was one of significant factors that explain the variation of total streamflow. However, it was not significant to explain the variation of the water supply reliability to 539 perturbations. It is explained in L18-28 in page 10.

(3) Climate response surface: The sampling of average precipitation and precipitation coefficient of variation (cv) is coarse (20% increments). I suggest sampling these factors at tighter increments. (4) The computational expense of conducting bottom-up climate risk assessment is mentioned several times in the text. How computationally intense is the Geum water system model to evaluate?

→ In revision, the perturbations for P_{avg} were adjusted to (e.g., -60% to +40% at a 10% interval). While we reached the same conclusions, this refinement would improve reliability of the logistic surfaces.

Role of GCM projections in the case study:

(1) GCMs are limited in their ability to simulate land/ocean/atmospheric mechanisms, especially those that take place at sub-grid scale resolution. This limits the information that can be credibly derived from projections for water resources planning. Precipitation coefficient of variation (CV), one of the climate variables used in the case study, is not well represented in GCMs so it is questionable to infer precipitation CV from GCM projections. This is why GCM projections are not shown on some of the response surfaces in Poff et al. 2015 (in response to page 3, Line 18-19 of this manuscript).

→ It is true that GCM projections are subject to significant uncertainty. It is not limited to P_{cv} . P_{avg} and T_{avg} may not be well captured by GCMs either. However, because of that reason, the bottom-up frameworks emerged by employing the stochastic tests imposing arbitrary climatic stresses on the hydrologic systems. Overlaying GCMs projections on the response surfaces is a common approach to gauge climate change risks in the bottom-up assessments. Superimposing GCMs on the logistic surfaces can provide information of future climate risks together with system robustness to climate change. It is discussed in L28 in page 14.

(2) This manuscript repeatedly mentions GCM counts as though GCM count in the feasible region on the climate response surface could be a decision criterion (e.g. page 3 line 19), and perhaps to some stakeholders it would be. However, this could also imply an attempt to quantify risk across the entire sampled climate space. Uncertainty quantification via ensembles of GCM projections is a challenging research question in its own right and would not be well treated by simply counting GCM projections from an arbitrary ensemble. Indeed, the point of bottom-up decision frameworks for climate risk management is avoiding this type of reliance on GCM projections with little scientific basis. Since this manuscript is designed to build on a bottom-up risk assessment framework, it is strange that so much emphasis is put on understanding performance under GCM projections in the text and figures. Titrating the framework: As mentioned above, it is not clear whether the logistic model is designed to model the risk of failing to mutually satisfy the eco-engineering performance thresholds or the risk of failing to meet one performance threshold. If the latter, the main technical contribution seems as appropriate for any single-objective climate response surface type risk assessment as for multi-objective climate response surface analyses, though it is applied here in a multi-objective climate response surface analysis. I would suggest the authors re-frame the analysis and revise the title to put the focus on the manuscript's main technical contribution, which is analyzing and communicating probabilistic information through a climate response surface (with an eco-engineering case study) rather than presenting a novel decision framework.

→ Considering this comment, the manuscript was retitled. By its nature, a multi-purpose response surface should have a narrower acceptable range than a single-purpose one. For better indications from the multi-purpose response surfaces, we just attempted to convert them to the logistic surfaces directly indicating the risk of system failure and then overlay climate projections. This point is highlighted in the revised manuscript, rather than focusing on the GCM counts.

Technical corrections (typing errors, etc.)

Word choice: The meaning of the terms “successive”, “risk of system failure”, and “sub-components” in the context of this analysis is not clear from the text.

→ As replied, in the revised manuscript, we did not use the terms “successive” and “sub-components”, but “risk of system failure” is still in use. It can be viewed as the probability of unsatisfactory performances throughout the manuscript.

Page 2, line 31: Whatley et al. 2014 should be Whateley et al. 2014 → We will globally check mistypos.

→ We globally checked the mistypos, and re-listed the references.

Page 3, section 5: “However, all assessments using the response surfaces have focused on the “expected performance” rather than risk of system failure” Is this true? I thought many decision scaling papers evaluated reliability, which is risk of failure.

→ Instead, we emphasized the uncertainty in the response surfaces in the introduction (L26 in page 2).

Figure 9: Labels on X axis would be clearer in words. Also, isolating the results of the analysis to GCM projections is totally counter-intuitive here. The point of bottom-up climate response surface analyses is to avoid relying on GCMs in climate risk management.

→ Figure 9 was removed in the revision. Instead, we explained the trade-off between the location E and the sub-basin 2 when considering the instreamflow requirement using the logistic regressions in Figure 7.

Figure 2: It is not clear where and how the logistic model comes into this framework based on Figure 2. Figures: None of the response surface figures include precipitation CV as one of the axes, though this is one of the sampled climate variables. The reasoning behind this should be clarified in the text.

→ Now, the EEDC framework is narratively described rather than using Figure.

5 **Incorporating the logistic regression into a decision-centric framework for probabilistic assessment of climate change impacts on a complex water system**
Assessing water supply capacity in a complex river basin under climate change using the logistic eco-engineering decision scaling framework

Daeha Kim¹, Jong Ahn Chun¹, Si-Jung Choi²

¹APEC Climate Center, Busan, 48058, South Korea

²Korea Institute of Civil Engineering and Building Technology, Gyeonggi-do, 10223, South Korea

Correspondence to: Si-Jung Choi (sjchoi@kict.re.kr)

10 ~~**Abstract.** Climate change is a global stressor that can undermine water management policies developed with the assumption of stationary climate, necessitating robust strategies for operating water infrastructures under uncertain climate and socioeconomic conditions. In this study, we modified the eco decision scaling framework to assess water supply and environmental reliabilities varying across a large river basin in response to changing climate exposures. The ordinary climate responses functions of the decision scaling framework were replaced with the logistic response surfaces against pre-defined thresholds to measure risks of non-successive outcomes indicated by individual climate projections. The logistic response surfaces of water supply performances and those of environmental reliabilities at sub-systems within the river basin were all combined to gauge potential risks of climate change from multiple perspectives. The case study for a large river basin in South Korea showed water supply reliabilities at the sub-basins were expected to be satisfactory against the water demand projections to 2030, while the human-demand-only operations could lower the environmental reliabilities for 2020-2039. To reduce the environmental risks, the stakeholders should accept increasing risks of unsatisfactory water supply at the sub-basins with small water demands. This study highlights that the logistic eco engineering decision scaling would better support risk-based decision-making processes from multiple perspectives by allowing users to measure potential risks of unsatisfactory outcomes together with visualization of various system responses to climatic stresses in a complex hydrologic system.~~

25 **Abstract.** Climate change is a global stressor that can undermine water management policies developed with the assumption of stationary climate. While the response-surface-based assessments provided a new paradigm for formulating actionable adaptive solutions, the uncertainty associated with the stress tests pose challenges. To address the risks of unsatisfactory performances in a domain of climate stresses, this study proposed to incorporate the logistic regression into a decision-centric framework. The proposed approach replaces the “responses surfaces” of the performance metrics typically used for
30 the decision scaling framework with the “logistic surfaces” that describes the risk of system failures against pre-defined

performance thresholds. As a case study, water supply and environmental reliabilities were assessed within the eco-engineering decision scaling framework for a complex river basin in South Korea. Results showed that human-demand-only operations in the river basin could result in water deficiency at a location requiring ecological flows. To reduce the environmental risks, the stakeholders should accept increasing risks of unsatisfactory water supply performance at the sub-basins with small water demands. This study suggests that the logistic surfaces could provide convenience to measure system robustness to climatic changes from multiple perspectives together with the risk information for decision-making processes.

1 Introduction

Climate change is a global stressor that poses prodigious challenges to long-term management of water resources. While water infrastructures have been constructed across the globe to sustain human livelihood and activities, those assets have been traditionally managed by heuristic operation policies developed under the assumption of stationary climate (Cosgrove and Loucks, 2015; Cully et al., 2016). However, the probabilistic behaviours of hydro-climatological variables hydrological processes, however, can be significantly altered by the warming atmosphere; thereby, the traditional heuristic management is expected to become increasingly vulnerable (Brown et al., 2015; Georgakakos et al., 2012). The adaptive operations may reduce risks from climatic change and variability (e.g., Xu et al., 2015; Eum and Simonovic, 2010), but are often difficult to be utilized due to deeply uncertain climate and socioeconomic conditions (Weaver et al., 2013; Steinschneider and Brown, 2012).

When formulating management solutions to non-stationary climate for a water system, an essential step is to assess impacts of climate change on its performance. For assessing impacts of climate change on water resources systems, the primary-An established method approach-for the impact assessment was to investigate outputs of relevant system models forced by projections of the general circulation models (GCMs) under hypothetical greenhouse gas (GHG) emission scenarios (Brown et al., 2012; Wilby and Dessai, 2010; e.g., Xu et al., 2015; Eum and Simonovic, 2010). Though it was possible to derive potential adaptive solutions from the given climate projections (e.g., Vano et al., 2010), the scenario led (or namely "top-down") approach resulted in underutilization of the achieved solutions in practice (Weaver et al., 2013; Brown and Wilby, 2012). This type of assessments takes the 'predict-then-act' paradigm for which the first prerequisite is accurate and sufficiently reliable predictions. However, substantial efforts are still necessary to deliver improvement in climatic predictions (Shapiro et al., 2010; Piao et al., 2010; Barron, 2009; Goddard et al., 2009; Doherty et al., 2009). This implies that previous scenario led assessments were conducted before the first prerequisite was sufficiently satisfied. The GCM projections, however, are often biased by inappropriate model formulations and/or imperfectly understood physical processes (Stevens and Bony, 2013; Deser et al., 2012; Dufresne and Bony, 2008; Stainforth et al., 2005). Thus, they may be subject to unacceptable contain unacceptably high uncertainty and potential risk costs for policymakers (Brown et al. 2012), leading to underutilization of GCM-led strategies (Weaver et al., 2013; Brown and Wilby, 2012).

~~Given the high risk costs contained in GCM led analyses, adaptive solutions from a small collection of GCM projections might be discarded by decision-makers' risk-aversion behaviours (Brown et al., 2012).~~

To overcome the weakness of ~~the scenario~~GCM-driven led strategies assessments in practical decision support, alternative ~~approaches- frameworks~~ within the 'robust decision' paradigm have emerged (e.g., Hadka et al., 2015; Whateley et al., 2014; Lampert and Groves, 2010). These decision-centric ~~(or namely "bottom up")~~ approaches seek robust solutions that can minimize adverse effects of climatic stresses on given hydrological systems of interest. Examples include the decision scaling (Brown et al., 2012), the dynamic adaptive policy pathways (Haasnoot et al., 2013), the real option analysis (Woodward et al., 2014), the Info-gap decision theory (Korteling et al., 2013), and the robust decision making (Lempert and Groves, 2010) among others. Whereas the ~~'predict-then-act' paradigm top-down framework~~ focuses on the most likely future conditions ~~that can to~~ maximize expected utility, the ~~bottom-up decision-centric~~ approaches pay attention to sensitivity (or vulnerability) of system performance to climatic stressors (Weaver et al., 2013; Brown et al., 2012). ~~Examples include the decision scaling (Brown et al., 2012), the dynamic adaptive policy pathways (Haasnoot et al., 2013), the real option analysis (Woodward et al., 2014), the Info-gap decision theory (Korteling et al., 2013), and the robust decision making (Lempert and Groves, 2010) among others.~~ These approaches first evaluate system performance under diverse climatic exposures (i.e., stress tests). Then, the GCM projections are simply used as indicators of system vulnerability in the future (i.e., impact assessment). ~~This risk-based~~This paradigm framework accepts the irreducible uncertainty in climate predictions as an inevitable part of long-term planning, and guides decision-makers toward low-regret strategies for sustainable system performance under non-stationary climate (Poff et al., 2016).

Nonetheless, the bottom-up approaches have several shortcomings that may mislead to regretful outcomes, since climate predictions are not the only uncertainty source in a decision-making process. Steinschneider et al. (2015b) argued that uncertainty stemming from hydrologic modelling (e.g., rainfall-runoff modelling and system optimizations) commonly used in the stress tests could be comparable to those from climate predictions. Kay et al. (2014) also emphasized the necessity of uncertainty allowances to be used alongside the response surfaces of flood risk indicators. These studies suggest that simplifications and assumptions necessary for the stress tests, which underpin the bottom-up assessment, could misguide decision-makers to inappropriate and/or untimely strategies, necessitating additional risk information of non-successive outcomes together with performance metrics projected by GCMs.

Furthermore, one may cast a concern that the response surface based approaches Among the decision-centric frameworks, the assessments based on the response functions of system performance have provided convenience to define decision thresholds at which adaptation actions are required (e.g., Kim et al., 2018; Steinschneider et al., 2015a; Turner et al., 2014; Whateley et al., 2014; Brown et al., 2012; Prudhomme et al., 2010) Prudhomme et al., 2010; Brown et al., 2012; Steinschneider et al., 2015a; Whateley et al., 2014). They developed the relationships between system performances and climatic stressors (hereafter referred to as the "response surfaces") via stress tests. Then, GCM projections were employed to indicate future system performance on the response surfaces. The response-surface-based methods have been refined to consider spatially varying system performance (e.g., Schlef et al., 2018) and multiple management objectives within a

hydrological system (e.g., Cully et al., 2016). They allowed efficient evaluation of climate change risks simply by comparing the performance metrics indicated by a collection of GCMs against pre-defined thresholds.

5 Nonetheless, uncertainty of the response surfaces cannot be neglected due to assumptions and simplifications associated with the stress tests (Kay et al., 2014). Indeed, Steinschneider et al. (2015b) argued that hydrological modelling and climatic variability may introduce uncertainty in the response surfaces as much as GCM projections. Kim et al. (2018) showed how climate change risks can be underestimated when a modelling scale was inappropriately chosen. Hence, over-reliance on the response surfaces of general performance metrics may misguide users to inappropriate and/or untimely adaptation policies. Importantly, the response surfaces have usually been developed with climatic shifts defined by long-term changes in statistical moments of weather observations (e.g., Kim et al., 2018; Poff et al., 2016; Steinschneider et al., 2015a; Whateley et al., 2014), even though they might insufficiently explain variation of chosen performance indicators. Whateley and Brown (2016) found that water supply system performance can be attributed mostly to uncertainty in internal climate variability over a time horizon of policy planning.

10 The prior studies imply that risks of system failures still exists even in the climate zone of satisfactory performance in the response surfaces. This uncertainty issue may be mended in part by evaluating the risks of system failures along with the response surfaces of expected performances. While it is possible to conduct stochastic uncertainty analyses with the stress tests (e.g., Steinschneider et al., 2015b; Whateley and Brown, 2016), this approach would require expensive computational costs even with modern computing power (Whateley et al., 2016). In this work, therefore, an efficient approach was proposed to evaluate the risks of system failures within a decision-centric framework. We simply incorporated the logistic regression into typical stress tests for the response-surface-based assessments. As a case study, here we provided a slightly modified version of the eco-engineering decision scaling framework (Poff et al., 2016) to explore the probabilities of system failures varying across a complex river system with two contrasting management purposes.

15 may over rely on the chosen performance indicator. If it is developed with a general performance metric of hydrologic systems (e.g., Turner et al., 2014), the response surface may not conceive failures at their sub-systems or those from other standpoints hidden behind successive general performance. The performance of water resources systems can vary across scales (e.g., entire system vs. sub-systems) and standpoints (e.g., for human demands vs. for environmental requirements), since practical management options are beyond the optimality of general performance due to uncertain hydrologic and socioeconomic conditions (Herman et al., 2014; Rosenberg, 2015). To overcome this weakness, Steinschneider et al. (2015a) expanded the decision scaling framework by developing multiple response surfaces of various indicators. Cully et al. (2016) embedded the multi-objective failure boundaries in the response surfaces of operational performances in a reservoir system. Schlef et al. (2017) investigated spatio-temporal variability of sub-components' vulnerability in a complex regulated river system.

25 A limitation of the abovementioned studies, however, is that users may face significantly increased dimensionality when many scales and standpoints are considered. If many adaptation options are preselected for the stress tests, increasing dimensionality of the response surfaces would become far more problematic. To this dimensionality problem, the eco-

5 decision-sealing framework (Poff et al., 2016) may be a solution. Poff et al. (2016) proposed to overlap multiple response surfaces representing engineering and ecological performances so as to identify climate zones within which all the performance criteria are mutually satisfied. This approach enables users to gauge the climatic tolerance of given systems from multiple perspectives. Likewise, one can evaluate system performances varying across scales and standpoints by integrating their response surfaces into one single climatic domain. Despite simplicity and usefulness of the eco-decision sealing, few studies have taken this flexible framework for assessing performance of water systems under non-stationary climate.

10 In this work, therefore, we attempted to assess impacts of climate change on water supply capacity of a regulated river basin using the eco-engineering decision-sealing framework in combination with the logistic regression analysis. Here, performance indicators varying across the complex river basin were evaluated using multiple logistic response surfaces to provide probabilities of successive outcomes in response to climate stressors. For the bottom-up assessment, we embedded a sequential optimization scheme in stochastic stress tests to quantify water supply reliabilities under diverse climate stresses. The performances of the entire system and its sub-components gained from the stress tests were visualized all together in a single climatic space for better understanding of the subsystem's responsive behaviours to climatic changes. Numerous GCM-projections were then superimposed on the combined response surface to evaluate future system performances under projected climate scenarios.

2-Description of the study site and data

2.1 Geum River Basin

20 The study site is the Geum River Basin located in the west central part of South Korea with a total area of 9,915 km² (Figure 1). The mean and the highest elevations in the river basin are 85 m and 1,596 m above the sea level, respectively. The mean basin slope is 16.7 % from the elevation profile. The total length of the main channel is approximately 402 km. The river basin has a semi-humid climate with monsoonal summer seasons. Wet air masses moving from the North Pacific make hot and humid summer seasons, whereas winter seasons are dry and cold due to the Siberian high pressure. Approximately, 60-70% of annual precipitation falls in the monsoonal summer seasons (June to September) (KMA, 2011). Streamflow in the river basin usually peaks in the middle of monsoon seasons by tropical or extra-tropical cyclones, while occasional precipitation events limitedly recharge the river basin during dry seasons (October to May). Snowmelt minimally influences streamflow variations due to small winter precipitation (Bae et al., 2008).

25 The Geum River Basin is officially divided into 14 sub-basins for administrative purposes along the geomorphological boundaries. The sub-basin areas vary between 120 and 1,856 km² with an average of 708 km². 60% of the river basin is covered by forests, while the agricultural areas account for 18%. The forest covers and agricultural lands in the 14 sub-basins occupy 33-83% and 4-6-42% of the sub-basin areas, respectively. The sub-basins with relatively large agricultural lands tend to have small forest covers. The urban areas are 5.2% of the river basin in total. According to the Korea Forest Service

(<http://forest.go.kr>), the soils across the Geum River Basin generally have moderate to high infiltration capacity, implying that the sub-surface processes significantly contribute to event flow generations.

Human interventions affect the flow regimes in the Geum River Basin. The main channel is regulated by two large dams serially connected for water supplies and flood controls. The Yongdam Dam located in the upper river basin has an effective storage capacity of 809 Mm^3 , while the Daecheong Dam at the middle of the main channel has a larger capacity of 1,040 Mm^3 . The water storages in both dams are delivered to several sub-basins through water distribution systems developed for municipal and industrial (M&I) water demands, making non-geomorphological human-made connectivity between the sub-basins. The two large dams supply water to the demand sectors in outside of the river basin through the distribution systems; hence, inter-basin water transfers may conflict with water demands within the river basin. During monsoon seasons, Yongdam and Daecheong Dams should reduce their storage limits by 137 Mm^3 and 250 Mm^3 for flood control, respectively. Additionally, many small-size local reservoirs are widespread across the river basin to sustain irrigated agriculture (mostly for planting paddy rice). Though 95% of the small reservoirs have minimal storage capacities below 1 Mm^3 , their gross capacity is more than 220 Mm^3 and thus significantly alters natural flow regimes. The total storage capacities of the agricultural reservoirs in the 14 sub-basins are from 1.1 Mm^3 to 100.9 Mm^3 with a median value of 12.5 Mm^3 . In each sub-basin, natural river flows and water transferred from the storage facilities (i.e., the agricultural reservoirs and dams) are consumed for agricultural and municipal and industrial (M&I) purposes. The water diverted for the M&I demands could return to the rivers, becoming available water for lower demand sectors.

For water resources system analyses, we simplified the complex river basin using a node and link network as shown in Figure 1. Each sub-basin was conceptualized as a node with natural water availability (i.e., natural runoff), storage capacity (i.e., water storage in the agricultural reservoirs), and water demands (i.e., agricultural and M&I water uses). The sub-basin nodes were connected by the stream links (the continuous lines). The two large dams were represented by the nodes only having storage capacities and located between the two adjacent sub-basins accordingly. The outside water demand sectors were represented by nodes with no natural flows and zero storage capacities. The human-made connections between the dams and the sub-basins are conceptualized by the separate links (the dashed lines) with conveyance limits.

2.2 Climatological data

We collected daily precipitation and maximum and minimum temperatures over South Korea at 3 km grid resolution for 1973–2015. The grid data were produced by interpolating synoptic observations at 60 stations in the automated surface observing system (ASOS) operated by the Korea Meteorological Administration. The point weather data were spatially interpolated by the Parameter Elevation Regression on Independent Slope Model (PRISM; Daly et al., 2008), and overestimated values were smoothed by the inverse distance method. Jung and Eum (2015) found improved performance of the combined method in South Korea via comparative evaluations to the original PRISM. For this study, the collected grid data were spatially aggregated with the sub-basin boundaries. For runoff simulations at the sub-basin nodes, we imposed

~~various hypothetical climatic stresses on the spatially aggregated precipitation and temperatures using a semi-parametric stochastic weather generator.~~

According to the grid data, the mean annual precipitation and temperature over the Geum River Basin for 1976–1995 were 1,245 mm and 11.7 °C, respectively. They have risen to 1,325 mm (+6.4%) and 12.2 °C (+0.5°C) during 1996–2015, providing an indication that atmospheric water supply and demand gradually increase over time. However, climatology within the river basin diverges between the sub-basins. The upper sub-basins at higher elevations tend to get wetter due to increasing precipitation, whereas rising temperatures seem to make the lower basins become drier (Kim, 2018).

2.3 Water demand data

The water demands for 2030 were taken as the reference demands to evaluate water supply capacity of the river basin. In South Korea, government-driven national water resources plans are legally developed for sustainable resources management for every bi-decadal period. The water resources plan for 2020 was first established in 2000 including water demand projections up to 2020 (MOCT, 2000), and has been revised three times to consider hydrologic and socioeconomic changes since the initial version (MOCT, 2006; MLTM, 2011; MOLIT, 2016). In the third version of the water resources plan for 2020 (MOLIT, 2016), the water demands across South Korea were re-projected up to 2030. By electronic correspondence (requested on Sep 26/2017), we achieved the demand data projected to 2030 given at 10-day intervals for each sub-basin in the Geum River Basin from the team leading the national water plan at the Korea Institute of Civil Engineering and Building Technology. We briefly describe about the water demand projections here, and the details are found in the third national plan for 2020 (MOLIT, 2016).

The agricultural and M&I demands are independently projected for the year of 2030 under the high, medium, and low demand scenarios. The agricultural demand within a sub-basin was estimated by the FAO Penman-Monteith equation (Allen et al., 1998). The potential evapotranspiration on each day of year was averaged across the observed periods. The effective rainfall was excluded to represent irrigation requirement. The mean irrigation requirement for each crop was multiplied by the planting area projected for 2030. The planting areas under the medium demand scenario were extrapolated by temporal trends in historical observations. The high demand scenario applied 3.5% additional increase to the standard projections, while the low demand scenario decreased the standard projections by 3.5%. On the other hand, the M&I demands were projected using historical water use records under hypothetical future growth rates and socioeconomic conditions. The medium scenario assumed 4.0% economic growth and 100% effectiveness of the water conservation programs in the future. For the high and low demand scenarios, 4.5% and 50% of growth rates and 3.5% and 150% effectiveness of the conservation programs were used, respectively. The three scenarios all expected decreasing water demands from 2016 to 2030 mainly due to declining rice-planting lands. In this study, the high demand scenario was chosen from a conservative perspective. The M&I demands at the two nodes out of river basin boundary were estimated by the water transfer records from the two dams for simplicity.

In addition, we collected the information of the minimum flow rates required for ecosystem sustainability, namely instream flows (Jowett, 1997), at seven locations within the river basin. The instream flows are determined by the experts' investigations into water quality and ecological conditions in the vicinity of major rivers in South Korea, and officially announced by the Ministry of Environment and the Ministry of Land, Infrastructure, and Transport (MOLIT, 2016). Though the human water demands (i.e., agricultural and M&I uses) are the first priority of the local and regional authorities in the Geum River Basin (MOLIT, 2016), they are recommended to consider the instream flows in water management. The human demands for the year of 2030 and the environmental requirements are summarized in Table 1. For water resources system modelling in this study, the 10-day demand data were aggregated into monthly values.

2.4 GCM projections under greenhouse gas concentration scenarios

We achieved daily projections of 25 GCMs (Table A1) from the archive of the Coupled Model Intercomparison Project Phase 5 (Taylor et al., 2012). Two representative concentration pathways (RCPs), RCP4.5 and RCP8.5, were selected to assess the water supply capacity of the river basin for the upcoming bi-decadal period of 2020-2039. RCP4.5 and RCP8.5 were used as scenarios of stabilized and increasing greenhouse gas concentrations frequently in climate change studies (e.g., Yan et al., 2015; Zhang et al., 2016; Moursi et al., 2017).

The 50 GCM projections (i.e., 25 GCMs \times 2 RCPs) were bias-corrected by the de-trended quantile mapping (DQM; Bürger et al., 2013; Eum and Cannon, 2017) that can preserve raw climate change signals given by GCMs. The DQM removes the long-term mean change in projected values first. After applying the ordinary quantile mapping (QM; e.g., Hwang and Graham, 2012) to the de-trended values, the removed trend is reintroduced to the bias-corrected projections. The de-trending procedure may prevent the exaggeration of raw climate change signals, which is a typical drawback of the ordinary QM. More details about DQM and related bias correction methods are available in Bürger et al. (2013), Cannon et al. (2015), and Eum and Cannon (2017). To correct the 50 GCM projections toward the spatial averaged precipitation and temperatures over the Geum River Basin, 1976-2005 and 2006-2009 were set as the reference and the projection periods, respectively.

3.2 Methodology

3.2.1 The logistic-eco-engineering decision scaling framework

The eco-engineering decision scaling (EEDS) framework (Poff et al., 2016) expanded the decision scaling (Brown et al., 2012) to consider stakeholders' multifaceted interests in the response surfaces. Iterative five-steps are required for this framework. Step 1 is to identify possible management options (O_1 and O_2), to select indicators of ecological and engineering performances (e.g., water supply reliability and ecological vulnerability), and to define user-specific thresholds under which the system performs unacceptably (θ_1 and θ_2). Step 2 is to build system models for the hypothetical stress tests. For water resources management, the system models may include a runoff model and a water allocation model. By exposing the system models to a wide range of hypothetical climatic stressors (x_1 and x_2), ecological and engineering performances can be

Formatted: Subscript

Formatted: Subscript

Formatted: Subscript

5 evaluated. In step 3, the response surfaces of engineering and ecological performances are developed with outcomes of the stress tests. For vulnerability analysis, the pre-defined thresholds (θ_1 and θ_2) are imposed on the response surfaces. Step 4 is to evaluate the management options with the size of the climatic zones satisfying the performance thresholds. In step 5, preferred decisions for the management options can be made. Or, if necessary, the assessment from step 1 to 4 can be repeated with new management options and/or different criteria.

In the EEDC framework, the key information would be the size of the climate zone mutually satisfying the engineering and ecological thresholds, since it measures overall system robustness to climate stresses. Decision-makers may prefer management options that can widen the mutual climate zone, if they are socio-economically viable. However, the system robustness is not the only criterion for selecting management options. In decision-making processes, questions can be raised such as “what if future climates will not fall within the mutual climate zone?” and “how much risks of system failures still exist within the climate zone that expects satisfactory performances?” Those questions can be answered by incorporating the logistic regression and a collection of GCM projections into the EEDC framework.

2.2 Incorporating the logistic regression into the stress tests

15 The stress tests in step 3 for the EEDC framework are intended to find expected performances per given climate exposures. By comparing the obtained performances against a pre-defined threshold, the climate exposures applied to the stress tests can be categorized into binary outcomes (i.e., 1 for satisfactory metrics and 0 for otherwise). With no needs of the homogeneity and normality assumptions, the logistic regression model allows to explain occurrences of the satisfactory performances with the sigmoid function of the climate exposures (x_i):

$$\pi = \frac{1}{1 + \exp[-(\beta_0 + \beta_1 x_1 + \beta_2 x_2 + \dots)]} \quad (1)$$

where, π is the probability of satisfactory performance, and β_j are the regression coefficients. Thus, $1 - \pi$ becomes the probability of unsatisfactory performance.

25 When two explanatory variables are chosen for x_i (e.g., changes in mean annual precipitation and temperature), it is possible to develop a 2-dimensional surface to describe variation of π within a climate domain. Hereafter, the surface of π will be referred to as the “logistic surface”. In this study, the logistic surfaces were used for the steps 3 and 4 of the EEDC framework in lieu of the response surfaces. The following example shows how to assess the risk of system failures together with robustness to climate stresses for a complex water system.

30 Figure 2 describes the logistic eco-engineering decision sealing framework that combines multiple responses of a hydrologic system to diverse climate exposures. While this concept is similar to the decision sealing (Brown et al., 2012; Steinschneider et al., 2015a), the eco-engineering decision sealing overlaps the response surfaces of multiple performance metrics to consider conflicting interests of stakeholders in decision-making processes. The size of the climate zone mutually satisfying

Formatted: Subscript

Formatted: Subscript

Formatted: Not Superscript/ Subscript

the multiple performance criteria enables to measure the system robustness to climate stressors from various perspectives. Valid hydrologic models are prerequisites to develop the response surfaces. According to the definition of climate change in IPCC (2007), climatic perturbations in this study are changes in the bi-decadal mean and variance in observed climatology. The first step of the bottom up impact assessment is to generate adequate sets of synthetic weather series perturbed by diverse climatic stresses for an exhaustive sensitivity analysis of system performance. By inputting a set of the generated weather series perturbed by user defined climate stresses to system models, the system behaviours can be simulated in response to the perturbations. If the stochastic stress tests are repeated with fairly large sets of climatic perturbations, the relationship between climate stresses and performance metrics of the user's interest can be developed. This relationship has been defined as the response surface (Kay et al., 2014), or the climate response function (Brown et al., 2012). Poff et al. (2016) developed multiple response surfaces for conflicting system performance indicators using the stochastic sensitivity analysis, and overlapped them all to identify the climatic zone mutually satisfying the stakeholder-driven thresholds. In this study, we slightly modified this framework by converting the response surfaces of performance metrics using the logistic regressions between binary outcomes against the threshold and corresponding climatic perturbations. This conversion allows users to estimate the probability of successive (or non successive) outcomes against the threshold. We defined the converted surfaces as the logistic response surface. In this study, water supply performance of the study river basin under two possible management policies was assessed using a classical optimization scheme for water resources management. With the optimized decision variables, we evaluated water supply reliabilities at each demands nodes of the conceptualised river basin model. The environmental reliabilities against the instream flows at the seven locations were evaluated together under each management policy. The logistic response surfaces were all overlapped to measure vulnerability of the sub-components to climate stresses from multiple perspectives. Details are following next.

3 Application: A case study for optimal water allocation in a complex water system

3.1 Study area

The case study area is the Geum River Basin located in the west-central part of South Korea with a total area of 9,915 km² (Figure 1). The mean and the highest elevations in the river basin are 85 m and 1,596 m above the sea level, respectively. The mean basin slope is 16.7%. The total length of the main channel is approximately 402 km. The river basin has a semi-humid climate with monsoonal summer seasons. Wet air masses moving from the North Pacific usually make hot and humid summer seasons, whereas winter seasons are dry and cold due to the Siberian high pressure. Approximately, 60-70% of annual precipitation falls in June to September (KMA, 2011); thus, river flows across the basin peaks in the middle of summer monsoon seasons. Snowmelt runoff minimally contributes to streamflow variations due to small winter precipitation (Bae et al., 2008).

5 The Geum River Basin is officially divided into 14 sub-basins for administrative purposes along the geomorphological boundaries. The sub-basin areas vary between 120 and 1,856 km² with an average of 708 km². 60% of the entire river basin is covered by forests, while agricultural areas account for 18%. The forest covers and agricultural lands within the 14 sub-basins occupy 33-83% and 4.6-42%, respectively. The sub-basins with relatively large agricultural lands tend to have small forest covers. The urban areas are 5.3% of the river basin in total. According to the Korea Forest Service (<http://forest.go.kr>), the soils across the Geum River Basin have moderate to high infiltration capacity, implying sub-surface runoff generations are dominant.

10 Human interventions affect the flow regimes in the Geum River Basin. The main channel is regulated by two large dams serially connected for water supplies and flood controls. The Yongdam Dam located in the upper river basin has an effective storage capacity of 809 Mm³, while the Daecheong Dam at the middle of the main channel has a larger capacity of 1,040 Mm³. Water storages in both dams are delivered to several sub-basins through water distribution systems developed for municipal and industrial (M&I) water demands, making non-geomorphological human-made connectivity between the sub-basins. The two large dams supply water to the demand sectors in outside of the river basin through the distribution systems; hence, inter-basin water transfers may conflict with water demands within the river basin. During monsoon seasons,
15 Yongdam and Dacheong Dams should reduce their storage limits by 137 Mm³ and 250 Mm³ for flood control, respectively. In addition, many small-size local reservoirs are widespread across the river basin to sustain irrigated agriculture (mostly for planting paddy rice). Though 95% of the small reservoirs have minimal storage capacities below 1 Mm³, their gross capacity is more than 320 Mm³ and thus considerably alters natural flow regimes. The total storage capacities of the agricultural reservoirs in the 14 sub-basins are from 1.1 Mm³ to 100.9 Mm³ with a median value of 12.5 Mm³. In each sub-basin, natural
20 river flows and water transferred from the storage facilities (i.e., the agricultural reservoirs and dams) are consumed for agricultural, and municipal and industrial purposes. The water diverted for the M&I demands could return to the rivers, becoming available water for lower demand sectors.

25 For water allocation modelling, we simplified the complex river system with a node-and-link network shown in Figure 1. Each sub-basin was conceptualized as a node with natural water availability (i.e., natural runoff), storage capacity (i.e., water storage in the agricultural reservoirs), and water demands (i.e., agricultural and M&I water uses). The sub-basin nodes were connected by the stream links (the continuous lines). The two large dams were represented by the nodes only having storage capacities and located between the two adjacent sub-basins accordingly. The outside water demands sectors were represented by nodes with no natural flows and zero storage capacities. The human-made connections between the dams and the sub-basins were conceptualized by separate links (the dashed lines) with conveyance limits.

3.2 Data collections

3.2.1 Climate and water demand data

Formatted: Heading 3

We collected daily precipitation and maximum and minimum temperatures over South Korea at 3-km grid resolution for 1973-2015. The grid data were produced by interpolating synoptic observations at 60 stations in the automated surface observing system (ASOS) operated by the Korea Meteorological Administration. The point weather data were spatially interpolated by the Parameter-elevation Regression on Independent Slope Model (PRISM; Daly et al., 2008), and overestimated values were smoothed by the inverse distance method. Jung and Eum (2015) found improved performance of the combined method in South Korea via comparative evaluations to the original PRISM. For the case study, the collected grid data were spatially aggregated with the sub-basin boundaries. The aggregated daily precipitation and temperature were perturbed by a stochastic weather generator for the stress tests, and then used to generate streamflow at the sub-basin nodes. According to the grid data, the mean annual precipitation and temperature over the Geum River Basin for 1976-1995 were 1,245 mm and 11.7 °C, respectively. They have risen to 1,325 mm (+6.4%) and 12.2 °C (+0.5°C) during 1996-2015, providing an indication that atmospheric water supply and demand gradually increase over time within the river basin.

The water demands for 2030 were taken as the reference demands to evaluate water allocation performance across the river basin. In South Korea, government-driven national water resources plans are legally developed for sustainable resources management for every bi-decadal period. The water resources plan for 2020 was first established in 2000 including water demand projections up to 2020 (MOCT, 2000), and has been revised three times to consider hydrologic and socioeconomic changes since the initial version (MOCT, 2006; MLTM, 2011; MOLIT, 2016). In the third version of the water resources plan for 2020 (MOLIT, 2016), the water demands across South Korea were re-projected up to 2030. By electronic correspondence (requested on Sep-26/2017), we obtained the demand data projected to 2030 given at 10-day intervals for the sub-basins and the two outside nodes directly linked to sub-basins from the team leading the national water plan at the Korea Institute of Civil Engineering and Building Technology. Among the high, standard, low demand scenarios given in MOLIT (2016), we chose the high demand scenario from a conservative perspective. More details about the demand projections are available in MOLIT (2016). The M&I demands at the two outside nodes connected with the two dams were estimated by the water transfer records for simplicity.

In addition, we collected the information of the minimum flow rates required for ecosystem sustainability, namely “instreamflows” (Jowett, 1997), at seven locations within the river basin. The instreamflows are determined by the experts’ investigations into water quality and ecological conditions in the vicinity of major rivers in South Korea, and officially announced by the Ministry of Environment and the Ministry of Land, Infrastructure, and Transport (MOLIT, 2016). Though the human water demands (i.e., agricultural and M&I uses) are the first priority of the local and regional authorities (MOLIT, 2016), they are recommended to consider the instreamflows for environmental sustainability. Table 1 summarizes the agricultural and M&I demands for the year of 2030 and the instreamflow requirements. For water allocation modelling, the demand data at 10-day interval were aggregated into monthly values.

3.2.2 Bias-corrected GCM projections

Daily precipitation and temperature projections of 25 GCMs (Table A1) were collected from the archive of the Coupled Model Intercomparison Project Phase 5 (Taylor et al., 2012). Two representative concentration pathways (RCPs), RCP4.5 and RCP8.5, were selected to assess the water supply capacity of the river basin for the upcoming bi-decadal period of 2020-2039. RCP4.5 and RCP8.5 were used as scenarios of stabilized and increasing greenhouse gas concentrations frequently in climate change studies (e.g., Yan et al., 2015; Zhang et al., 2016; Moursi et al., 2017).

The 50 GCM projections (i.e., 25 GCMs×2 RCPs) were bias-corrected by the de-trended quantile mapping (DQM; Bürger et al., 2013; Eum and Cannon, 2017) that can preserve raw climate change signals given by GCMs. The DQM removes the long-term mean change in projected values first. After applying the ordinary quantile mapping (QM; e.g., Hwang and Graham, 2013) to the de-trended values, the removed trend is reintroduced to the bias-corrected projections. The de-trending procedure may prevent the exaggeration of raw climate change signals, which is a typical drawback of the ordinary QM. More details about DQM and related bias correction methods are available in Bürger et al. (2013), Cannon et al. (2015), and Eum and Cannon (2017). To correct the 50 GCM projections toward the spatial averaged precipitation and temperatures over the Geum River Basin, 1976-2005 and 2006-2099 were set as the reference and the projection periods, respectively.

3.3 Stress tests for water allocation performances

The stress tests were conducted for optimal water allocations in the node-and-link system. The 14 sub-basins are forced by atmospheric drivers (i.e., precipitation and temperature) to generate natural streamflow. The generated streamflows are regulated to meet the water demands and instreamflow requirements. The operations should be constrained by geomorphological and management conditions. We used a conceptual runoff model and an optimization model for evaluating water supply and ecological performances with stochastic weather series perturbed by hypothetical climate stresses.

3.2-3.1 Generating climate-stress-induced weather series

The stochastic weather generator (WG) by Steinschneider and Brown (2013) was employed to produce plausible daily precipitation and temperature sequences with climatic perturbations (i.e., generating climate stresses). Several bottom-up assessments successfully used this model to evaluate performance of hydrologic systems under varying climate stresses (e.g., Whateley et al., 2014; Steinschneider et al., 2015b).

Two stochastic models are combined in the semi-parametric WG. The wavelet autoregressive model proposed by Kwon et al. (2007) first generates annual precipitation series spatially-averaged within a region of interest for a desired length (20 years in this study). The wavelet components of the annual precipitation series are extended by the autoregressive model to embed the low-frequency structure inherent in observations. Then, daily weather series conditioned by the random annual precipitation are simulated by the Markovian bootstrap resampler of Apipattanavis et al. (2007). In this process, the daily

Formatted: Heading 3

Formatted: Normal

5 observations are resampled by the k-nearest-neighbour scheme and the precipitation occurrence series generated by the standard Markovian process (e.g., Wilks, 1998). The weather data at multiple locations within the region of interest are sampled together for spatial coherence. As the final step, the mean and variance of stochastic precipitation series are adjusted by the ordinary QM to impose climatic perturbations stresses. The temperature series are simply perturbed by adding a temperature differential. Further in-depth details about the stochastic WG are found in Steinschneider and Brown (2013).

To examine the water supply performance under climatic stresses, we generated ~~343-539~~ sets of precipitation and temperature time series spatially coherent between the 14 sub-basins. The perturbations imposed on the precipitation time series were changes in the mean of non-zero daily precipitation and its coefficient of variance (CV). The ~~applied mean and CV-changes of precipitation~~ were from ~~-4060%~~ to ~~+8040%~~ at ~~2010%~~ increments relative to the observations for 1973-2015, ~~while the CV changes were from -40% to +80% at 20% increments, respectively~~ (i.e., ~~711~~×7 perturbations for precipitation). The temperature time series were perturbed by adding 0-6 °C at 1°C increments (i.e., 7 perturbations for temperature). ~~Thus, The-the~~ total number of the climatic perturbations ~~is-was~~ ~~711~~×7×7=~~343539~~. The ~~343-539~~ sets of climate-stress-induced weather series were input to a rainfall-runoff model to quantify natural water flows at the sub-basins. ~~To develop the logistic response surfaces, each weather series generated by the WG were summarized by three bi-decadal properties of the mean annual precipitation (P_{avg}), the CV of daily precipitation (P_{cv}), and the mean annual temperature (T_{avg}).~~

3.3.2 Simulating natural runoff at the sub-basin nodes

A simple rainfall-runoff model, GR4J (Perrin et al., 2003), was ~~utilized-used~~ to simulate natural flows at the sub-basins nodes. GR4J has been frequently ~~adopted-employed in many studies for various purposes~~ under diverse climates, such as parameter regionalization (e.g., Oudin et al., 2010), predicting flow durations (e.g., Zhang et al., 2015), and low flow estimations (e.g. Demirel et al., 2015) among many others. ~~The four free parameters of GR4J uses four conceptual parameters to describe conceptualize~~ functional behaviours of a watershed in response to lumped precipitation and potential evapotranspiration (PET) inputs. The ~~free~~ parameters implicitly explain soil water storage, groundwater exchange, routing storage, and excess runoff generations within a watershed. The parsimonious structure of GR4J poses relatively small equifinality problem in parameter calibration and regionalization (Oudin et al., 2008; Perrin et al., 2007). Perrin et al. (2003) provides the computation procedures in detail.

In ~~the case this~~ study, a proximity-based regionalization was applied for parameter identification, because almost no natural streamflow observations are available at the outlets of the sub-basins. The operational inflow records at the Yongdam Dam were the only applicable observations for parameter calibration at the sub-basin 3001. For the other sub-basins, the parameter sets were transferred from neighbouring watersheds assessed in Kim et al. (2017). Kim et al. (2017) comparatively assessed performance of the proximity-based parameter transfer in comparison to several alternative methods, concluding that spatial proximity well captured functional similarity between 45 gauged watersheds in South Korea. The mean Nash-Sutcliffe efficiency (NSE) was 0.53 with a standard deviation of 0.41, when transferring the parameter sets of five neighbouring catchments calibrated with observed hydrographs (Kim et al., 2017). Hence, for the 13 sub-basins from 3002

Formatted: Heading 3

to 3014, natural flows were simulated with the transferred parameter sets from five nearby gauged watersheds, while flows at the sub-basin 3001 were generated by the parameters calibrated against the inflow data. The five runoff simulations were averaged for the sub-basins in which the regionalization scheme was used. The parameter set calibrated against the inflow records ~~during 2007-2015~~ for the sub-basin 3001 yielded a NSE value of 0.62 ~~for 2007-2015~~. The daily natural flows simulated by GR4J with the ~~343-539~~ stochastic weather sets were temporally aggregated at monthly values for water ~~allocation modelling resources system analyses~~.

~~3.3.4.3 Water allocation modelling~~ ~~Evaluating water supply and environmental reliabilities~~

The total water availability in the river basin during a certain month is water storages in the dams and reservoirs at the end of the previous month plus the natural flows at the sub-basins in the current month. Some of the available water is again kept in the storage facilities for supplying water in upcoming months. Thus, operators' decisions on water storages in each month recursively affect supply performance in the river basin through a bi-decadal period. A monthly sequential optimization model was used to determine amounts of the water storages and ~~uses consumptions~~ at each sub-basin. The operators should to minimize water deficiency during a current month, while the water storages need to be maximized for water ~~availability supplies~~ in upcoming months. We assumed that the two conflicting objectives are equally important for the operators. Hence, the objective function to determine water supplies and storages at the nodes for a particular month was:

$$\text{Minimize } \frac{\sum D_i - \sum S_i}{\sum D_i} - \frac{\sum V_i - \sum C_i}{\sum C_i} \quad (4a2a)$$

$$D_i = DA_i + DM_i \quad (4b2b)$$

$$S_i = SA_i + SM_i \quad (4c2c)$$

where, D_i is the total demand, S_i is the total supply, V_i is the water storage, and C_i is the storage capacity (C_i) at node i . SA_i and SM_i are agricultural and M&I water supplied for agricultural (DA_i) and M&I demands (DM_i) at node i , respectively. The total water demand at each node (D_i) is the sum of agricultural demand (DA_i) and M&I demand (DM_i). Likewise, the water supply at each node is divided into agricultural supply (SA_i) and M&I supply (SM_i).

The monthly optimizations were subject to constraints. The water supply (S_i) to a demand node was limited by water availability, which is the sum of natural flow at the node in the current month, flows from other nodes via the stream and the human-made links in the current month, and water storage at the node in the previous month. Water surplus at the nodes was not allowed (i.e., $S_i \leq D_i$). The water remained after supplies and storage at a sub-basin node should be discharged from the node through the channel network. The water storage at each node is constrained by its storage capacity ($V_i \leq C_i$). The water transfers through the human-made links were only supplied for M&I demands of destination nodes, and were limited by the conveyance capacity ($40 \text{ Mm}^3 \text{ month}^{-1}$). The agricultural and M&I demands were of equal priorities in optimizations.

Formatted: Heading 3

Using ~~With~~ 20-year-long natural flows per climatic perturbation, we determined SA_i , SM_i , and V_i month by month using the global optimization tool “fmincon” in the Matlab software. Since V_i values determined for a month become water availability for its next month, optimizations for 240 months interplay sequentially. To consider the return flows, we followed the ~~hypotheses-assumptions~~ in the water plan for 2020 (MOLIT, 2016). Simply, 65% of the M&I water use at each node was assumed to return and become available water for following nodes, while no return flows after agricultural uses were considered in the water plan due to high water use efficiency.

3.3.4 Evaluating water supply and ecological performances

Using the optimized SA_i , SM_i , and V_i values, water supply performances at the demand nodes were measured for the given 20-year-long stress-imposed weather series. For each ~~demand-sub-basin node-of-the-node-and-link-network~~, we measured the water supply reliability ($\rho_{s,i}$) defined as the probability of satisfactory supply against 99% of the monthly demands:

$$\rho_{s,i} = \text{prob} [S_i \geq 0.99D_i] \quad (2)$$

The amount of water passing the seven locations with the instream-flow requirements can be also calculated using the decision variables and the natural flows. The environmental reliability at a instreamflow location j ($\rho_{e,j}$) was evaluated by:

$$\rho_{e,j} = \text{prob} [F_j \geq F_{\min,j}] \quad (3)$$

where, F_j and $F_{\min,j}$ are the flow passing location j and the instream flows required for ecosystem sustainability at the location, respectively.

In total, water reliabilities at ~~18-the 14~~ demand nodes (14 sub-basins ~~and 4 demand nodes out of the basin~~) and the 7 locations requiring instreamflows the environmental flows were evaluated for each climatic perturbation. These ~~25-21 sets of~~ performance indicators ~~and corresponding climatic perturbation~~ were used to develop the logistic response functions for each sub-basin node and instreamflow location with corresponding climate stress of system performance to climatic stressors. To develop the logistic surfaces, we assumed that the stakeholder-driven thresholds for $\rho_{s,i}$ and $\rho_{e,j}$ were 0.95 and 0.70, respectively. the 539 sets of P_{avg} , P_{cv} , and T_{avg} that represent the perturbed weather series were categorized into zero and one against the two thresholds for the logistic regressions.

3.5 Developing logistic climate response functions

~~We used the logistic regression analyses to identify responsive behaviours of system performance to bi decadal climatic stresses. With no needs of the homogeneity and normality assumptions, the logistic regression model can explain~~

Formatted: Heading 3

occurrences of a probabilistic process with relevant independent variables by assuming a linear relationship between the logit of the explanatory variables and binary responses (e.g., Lee et al. 2016). We categorized the water supply and environmental reliabilities gained from the stress tests into binary outcomes (i.e., satisfactory or non-satisfactory against a threshold). The binary outcomes corresponding to the 343 climatic perturbations were explained by the logistic equation:

$$\pi = \frac{1}{1 + \exp[-(\beta_0 + \beta_1 X_1 + \beta_2 X_2 + \dots)]} \quad (4)$$

where, π is the probability of successive outcomes, β_i are the regression coefficients, and X_i are explanatory variables.

Each weather series generated by the WG could be summarized with three bi-decadal climatic properties of the mean annual precipitation (P_{avg}), the CV of daily precipitation (P_{cv}), and the mean annual temperature (T_{avg}). P_{avg} , P_{cv} , and T_{avg} were used as the candidate explanatory variables.

~~In our sensitivity analysis, the climatic bounds distinguishing between successive and non-satisfactory performances were found at $\pi=95\%$ for the sub-components of the study river basin. We combined all the boundaries developed by the logistic regressions into a single climate domain. The GCM projections for 2020-2039 were overlaid on the domain to assess impacts of greenhouse gas emissions on the water supply and environmental reliabilities.~~
Description of the study site and data

2.1 Geum River Basin

The study site is the Geum River Basin located in the west-central part of South Korea with a total area of 9,915 km² (Figure 1). The mean and the highest elevations in the river basin are 85 m and 1,596 m above the sea level, respectively. The mean basin slope is 16.7 % from the elevation profile. The total length of the main channel is approximately 402 km. The river basin has a semi-humid climate with monsoonal summer seasons. Wet air masses moving from the North Pacific make hot and humid summer seasons, whereas winter seasons are dry and cold due to the Siberian high pressure. Approximately, 60-70% of annual precipitation falls in the monsoonal summer seasons (June to September) (KMA, 2011). Streamflow in the river basin usually peaks in the middle of monsoon seasons by tropical or extra-tropical cyclones, while occasional precipitation events limitedly recharge the river basin during dry seasons (October to May). Snowmelt minimally influences streamflow variations due to small winter precipitation (Bae et al., 2008).

The Geum River Basin is officially divided into 14 sub-basins for administrative purposes along the geomorphological boundaries. The sub-basin areas vary between 120 and 1,856 km² with an average of 708 km². 60% of the river basin is covered by forests, while the agricultural areas account for 18%. The forest covers and agricultural lands in the 14 sub-basins occupy 33.83% and 4.6-42% of the sub-basin areas, respectively. The sub-basins with relatively large agricultural lands tend to have small forest covers. The urban areas are 5.3% of the river basin in total. According to the Korea Forest Service (<http://forest.go.kr>), the soils across the Geum River Basin generally have moderate to high infiltration capacity, implying that the sub-surface processes significantly contribute to event flow generations.

Human interventions affect the flow regimes in the Geum River Basin. The main channel is regulated by two large dams serially connected for water supplies and flood controls. The Yongdam Dam located in the upper river basin has an effective storage capacity of 809 Mm³, while the Daecheong Dam at the middle of the main channel has a larger capacity of 1,040 Mm³. The water storages in both dams are delivered to several sub-basins through water distribution systems developed for municipal and industrial (M&I) water demands, making non-geomorphological human-made connectivity between the sub-basins. The two large dams supply water to the demand sectors in outside of the river basin through the distribution systems; hence, inter-basin water transfers may conflict with water demands within the river basin. During monsoon seasons, Yongdam and Daecheong Dams should reduce their storage limits by 137 Mm³ and 250 Mm³ for flood control, respectively. Additionally, many small-size local reservoirs are widespread across the river basin to sustain irrigated agriculture (mostly for planting paddy rice). Though 95% of the small reservoirs have minimal storage capacities below 1 Mm³, their gross capacity is more than 320 Mm³ and thus significantly alters natural flow regimes. The total storage capacities of the agricultural reservoirs in the 14 sub-basins are from 1.1 Mm³ to 100.9 Mm³ with a median value of 12.5 Mm³. In each sub-basin, natural river flows and water transferred from the storage facilities (i.e., the agricultural reservoirs and dams) are consumed for agricultural and municipal and industrial (M&I) purposes. The water diverted for the M&I demands could return to the rivers, becoming available water for lower demand sectors.

For water resources system analyses, we simplified the complex river basin using a node and link network as shown in Figure 1. Each sub-basin was conceptualized as a node with natural water availability (i.e., natural runoff), storage capacity (i.e., water storage in the agricultural reservoirs), and water demands (i.e., agricultural and M&I water uses). The sub-basin nodes were connected by the stream links (the continuous lines). The two large dams were represented by the nodes only having storage capacities and located between the two adjacent sub-basins accordingly. The outside water demands sectors were represented by nodes with no natural flows and zero storage capacities. The human-made connections between the dams and the sub-basins are conceptualized by the separate links (the dashed lines) with conveyance limits.

2.2 Climatological data

We collected daily precipitation and maximum and minimum temperatures over South Korea at 3 km grid resolution for 1973-2015. The grid data were produced by interpolating synoptic observations at 60 stations in the automated surface observing system (ASOS) operated by the Korea Meteorological Administration. The point weather data were spatially interpolated by the Parameter-elevation Regression on Independent Slope Model (PRISM; Daly et al., 2008), and overestimated values were smoothed by the inverse distance method. Jung and Eum (2015) found improved performance of the combined method in South Korea via comparative evaluations to the original PRISM. For this study, the collected grid data were spatially aggregated with the sub-basin boundaries. For runoff simulations at the sub-basin nodes, we imposed various hypothetical climatic stresses on the spatially aggregated precipitation and temperatures using a semi-parametric stochastic weather generator.

5 According to the grid data, the mean annual precipitation and temperature over the Geum River Basin for 1976-1995 were 1,245 mm and 11.7 °C, respectively. They have risen to 1,325 mm (+6.4%) and 12.2 °C (+0.5°C) during 1996-2015, providing an indication that atmospheric water supply and demand gradually increase over time. However, climatology within the river basin diverges between the sub-basins. The upper sub-basins at higher elevations tend to get wetter due to increasing precipitation, whereas rising temperatures seem to make the lower basins become drier (Kim, 2018).

2.3 Water demand data

10 The water demands for 2030 were taken as the reference demands to evaluate water supply capacity of the river basin. In South Korea, government-driven national water resources plans are legally developed for sustainable resources management for every bi-decadal period. The water resources plan for 2020 was first established in 2000 including water demand projections up to 2020 (MOCT, 2000), and has been revised three times to consider hydrologic and socioeconomic changes since the initial version (MOCT, 2006; MLTM, 2011; MOLIT, 2016). In the third version of the water resources plan for 2020 (MOLIT, 2016), the water demands across South Korea were re-projected up to 2030. By electronic correspondence (requested on Sep 26/2017), we achieved the demand data projected to 2030 given at 10-day intervals for each sub-basin in the Geum River Basin from the team leading the national water plan at the Korea Institute of Civil Engineering and Building Technology. We briefly describe about the water demand projections here, and the details are found in the third national plan for 2020 (MOLIT, 2016).

15 The agricultural and M&I demands are independently projected for the year of 2030 under the high, medium, and low demand scenarios. The agricultural demand within a sub-basin was estimated by the FAO Penman-Monteith equation (Allen et al., 1998). The potential evapotranspiration on each day of year was averaged across the observed periods. The effective rainfall was excluded to represent irrigation requirement. The mean irrigation requirement for each crop was multiplied by the planting area projected for 2030. The planting areas under the medium demand scenario were extrapolated by temporal trends in historical observations. The high demand scenario applied 3.5% additional increase to the standard projections, while the low demand scenario decreased the standard projections by 3.5%. On the other hand, the M&I demands were projected using historical water use records under hypothetical future growth rates and socioeconomic conditions. The medium scenario assumed 4.0% economic growth and 100% effectiveness of the water conservation programs in the future. For the high and low demand scenarios, 4.5% and 50% of growth rates and 3.5% and 150% effectiveness of the conservation programs were used, respectively. The three scenarios all expected decreasing water demands from 2016 to 2030 mainly due to declining rice planting lands. In this study, the high demand scenario was chosen from a conservative perspective. The M&I demands at the two nodes out of river basin boundary were estimated by the water transfer records from the two dams for simplicity.

25 In addition, we collected the information of the minimum flow rates required for ecosystem sustainability, namely in-stream flows (Jowett, 1997), at seven locations within the river basin. The in-stream flows are determined by the experts' investigations into water quality and ecological conditions in the vicinity of major rivers in South Korea, and officially

announced by the Ministry of Environment and the Ministry of Land, Infrastructure, and Transport (MOLIT, 2016). Though the human water demands (i.e., agricultural and M&I uses) are the first priority of the local and regional authorities in the Geum River Basin (MOLIT, 2016), they are recommended to consider the instream flows in water management. The human demands for the year of 2030 and the environmental requirements are summarized in Table 1. For water resources system modelling in this study, the 10-day demand data were aggregated into monthly values.

2.4 GCM projections under greenhouse gas concentration scenarios

We achieved daily projections of 25 GCMs (Table A1) from the archive of the Coupled Model Intercomparison Project Phase 5 (Taylor et al., 2012). Two representative concentration pathways (RCPs), RCP4.5 and RCP8.5, were selected to assess the water supply capacity of the river basin for the upcoming bi-decadal period of 2020-2039. RCP4.5 and RCP8.5 were used as scenarios of stabilized and increasing greenhouse gas concentrations frequently in climate change studies (e.g., Yan et al., 2015; Zhang et al., 2016; Moursi et al., 2017).

The 50 GCM projections (i.e., 25 GCMs \times 2 RCPs) were bias-corrected by the de-trended quantile mapping (DQM; Bürger et al., 2013; Eum and Cannon, 2017) that can preserve raw climate change signals given by GCMs. The DQM removes the long-term mean change in projected values first. After applying the ordinary quantile mapping (QM; e.g., Hwang and Graham, 2013) to the de-trended values, the removed trend is reintroduced to the bias-corrected projections. The de-trending procedure may prevent the exaggeration of raw climate change signals, which is a typical drawback of the ordinary QM. More details about DQM and related bias correction methods are available in Bürger et al. (2013), Cannon et al. (2015), and Eum and Cannon (2017). To correct the 50 GCM projections toward the spatial-averaged precipitation and temperatures over the Geum River Basin, 1976-2005 and 2006-2009 were set as the reference and the projection periods, respectively.

4 Results

4.1 Evaluating water supply reliability performance at the sub-basins using the logistic response surfaces

The stress tests that forced the system models (i.e., GR4J and the optimization model) by the perturbed weather series produced 539 sets of reliabilities for each sub-basin and each location of instreamflow. Figure 3-2 displays the scatter plots between the three explanatory variables (P_{avg} , P_{cv} , and T_{avg}) and water supply reliability (ρ_s) at the sub-basin 3001 and corresponding changes in P_{avg} , P_{cv} , and T_{avg} relative to 1996-2015, collected from 343 sets of the sequential optimizations.

We preliminarily checked statistical significance of the explanatory variables using the linear multiple regression multiple linear regressions. The changes in P_{avg} and T_{avg} were of very high significance, the most significant to explain variation of the ρ_s values (p-values $< 10^{-16}$) followed by T_{avg} (p-value $< 10^{-13}$), whereas the change in P_{cv} was insignificant of a low significance below 5% level (p-value = 0.28744). This implies This indicates that the bi-decadal water supply reliability is generally determined by variations of the mean total precipitation and the mean temperature for a bi-decadal period. Though

Formatted: Subscript

higher precipitation variability (P_{cv}) could generate more direct runoff across the river basin, indicates more intensified rainfall events generating larger direct runoff, storage capacities of the agricultural reservoirs and the dams seem to dampen nullify the effects-impacts of P_{cv} changes on the variation of water supply reliability, ρ_s . The preliminary regression analysis led us to an indication-a hypothesis that the two explanatory variables changes in P_{avg} and T_{avg} could sufficiently capture the variation of water supply performance-reliabilities across the demand nodes river basin.

The linear regression between (P_{avg} , T_{avg}) and the ρ_s values can show responses of a system performance to climatic stresses. Figure 4a-3a illustrates the regression function surface between the ρ_s values and changes in P_{avg} and T_{avg} changes relative to 1996-2015 ($R^2 = 0.90, 0.93$), on which the collection of 50 GCM projections was overlaid. All-Most of the 50 GCMs expected that ρ_s at the sub-basin 3001 would be greater than 0.95 for 2020-2039. This type of response surfaces between expected performance and hypothetical climatic stresses have been commonly used in the decision-centric bottom-up assessments (e.g., Brown et al., 2012; Whateley et al., 2014; Turner et al., 2014). Figure 3c indicate that ρ_s at the sub-basin 3001 could be less than 0.95, if P_{avg} decreases by 30% approximately. The ρ_s values varied significantly even with zero decrease in P_{avg} , indicating that there might be the risk of unsatisfactory supply performance even with no changes in P_{avg} .

The risk of $\rho_s < 0.95$ could be evaluated by the logistic surface shown in Figure 3b. The sigmoid functions fitted to binary outcomes categorized against the threshold of $\rho_s > 0.95$ (Figure 3d) could provide approximate probabilities of $\rho_s > 0.95$ (hereafter referred to as $\pi_{0.95}$) at the sub-basin 3001. $\pi_{0.95}$ declined with rising temperatures, since water availability was reduced by evaporation losses. On the other hand, the logit function fitted to the binary outcomes categorized by a threshold enables to estimate the probability that system performance would be successive. As shown in Figure 4b, we developed the logistic response surface using the 343 binary outcomes against a threshold of $\rho_s = 0.95$ and corresponding T_{avg} and P_{avg} values for the sub-basin 3001 (McFadden $R^2 = 0.84$). The $\pi_{0.95}$ values indicated by The the 50 individual GCMs predicted the probability of $\rho_s > 0.95$ (hereafter referred to as $\pi_{0.95}$) with a ranged between 74 and 99% range of 78-99% for 2020-2039. A lower $\pi_{0.95}$ implies a higher risk that the optimal water management would yield unsatisfactory supply reliability of $\rho_s \leq 0.95$. Though the GCMs overlaid on the ordinary response surface (Figure 4a) seemingly expect 0.95 or greater ρ_s for 2020-2039, the logistic response surface (Figure 4b) implies that $\pi_{0.95}$ would decrease from 99% to 95% with the same climate projections. It should be noted that the climatic bound for $\rho_s = 0.95 > 0.95 =$ in the ordinary response surface (dotted-dashed lines in Figure 43a and b) has the risk of $\rho_s < 0.95$ at 40-60% of chances on the logistic surfaces. It seems that there still exist considerable risks of unsatisfactory performances on the zone of satisfactory performance in Figure 3a, corresponds to only 45-65% of $\pi_{0.95}$. Hence, a user of the logistic response surface may perceive a higher climate change risk than those who gauge system performance with the ordinary response surface.

Likewise, For each demand node, we developed fitted the logistic response functions sigmoid functions to of the binary outcomes against the threshold of $\rho_s = > 0.95$ for the other sub-basins, using the sequential optimization results, and found the climatic bounds at which $\pi_{0.95}$ was 95%. Figure 5-4 displays shows the climatic bounds at which $\pi_{0.95} = 95\%$ for each sub-basin of $\pi_{0.95} = 95\%$ for the all demand nodes together. The sub-basin 3001 was of the highest bound among the 14 sub-basins, indicating that the uppermost sub-basin is the most vulnerable to changes in P_{avg} and T_{avg} . 15 GCMs were located

Formatted: Subscript

Formatted: Not Superscript/ Subscript

Formatted: Not Superscript/ Subscript

Formatted: Subscript

Formatted: Subscript

below the climate boundary of the sub-basin 3001. On the contrary, the boundary of the sub-basin 3012 was the lowest. For every GCM projections, $\pi_{0.95}$ at the sub-basin 3012 was larger than 99%. The sub-basins with limited connections to the upper sub-basins tend to have higher climatic bounds of $\pi_{0.95} = 95\%$. The lower sub-basins receiving streamflow generated by the upper sub-basins were likely to withstand stronger climate stresses, even though they have relatively large agricultural demands.

The climatic bounds for the demand nodes were all lower than the bound of $\pi_{0.95} = 95\%$ for the total water demands in the entire basin, indicating that operations toward minimizing overall water deficiency across the river basin may not force local unsatisfactory performance at the demand nodes. However, vulnerability to climatic stresses differs between the demand nodes. The sub-basin 3001 (the uppermost demand node) seems to be exposed to the highest climate change risks. It had the smallest climate zone for 95% or higher $\pi_{0.95}$, and the P_{avg} range for $\pi_{0.95} > 95\%$ sensitively declined with rising T_{avg} . The second vulnerability was found at the external demand node receiving water from the Yongdam Dam, which stores streamflow from the sub-basin 3001. On the contrary, the lowermost node (sub-basin 3014) has the largest climate zone for $\pi_{0.95} > 95\%$. Even with 40% reduction in P_{avg} , the sub-basin 3014 would be able to meet the threshold of $\rho_e = 0.95$ with 95% or a higher $\pi_{0.95}$. Its P_{avg} range for $\pi_{0.95} > 95\%$ was almost insensitive to rising T_{avg} . This is because the lower sub-basins below the Daecheong Dam could receive streamflow discharged from the upper sub-basins; thereby, they could withstand much stronger climatic stresses despite their high agricultural demands.

4.2 Evaluating reliability against the instream flows Environmental reliability against the instreamflow requirements

The monthly flows at the seven locations requiring the instream flows were calculated with the decision variables obtained from the optimizations and the given natural flow estimates. We compared the modelled flows at the 7 locations of instreamflow against the minimum requirements, and evaluated the environmental reliabilities (i.e., ρ_e) at each location. Figure 6-5 shows the box plots of ρ_e values at the seven locations in response to the 343-539 climate perturbations. While ρ_e values at all the locations decreased as climate became drier, the location E was seems to be the most vulnerable. Even with no changes in P_{avg} and T_{avg} , the outflows from the sub-basin 3011 were often less than the minimum requirement, implying that ecosystems near the location E might be currently undermined by the large agricultural and M&I demands at the sub-basin 3011. If P_{avg} was declined/decreased by 20% and T_{avg} rose by 3°C, ρ_e at the location E would fall below 0.5. On the other hand, streamflow at the location D perfectly satisfied the minimum instreamflow requirement under the same stress. Despite the second-largest M&I demands at the sub-basin 3009, water transfers from the two large dams could deliver sufficient water supplies. 65% of the water supplies for M&I demand was supposed to return to the stream network and became streamflow to meet the instream-flow requirement at the location D. Although both sub-basins 3009 and 3011 have limited geomorphological connectivity to the upper sub-basins, their demand components and linkages to the two large dams made the significant difference between their ρ_e values.

We developed the logistic response surfaces with binary outcomes against the threshold of $\rho_e \geq 0.70$ at which the instreamflow requirement at the location E were satisfied in the optimization model under no climate stresses (i.e., no

changes in P_{avg} and T_{avg} relative to 1996-2015) and corresponding (T_{avg}, P_{avg}) pairs. The threshold $\rho_e = 0.70$ was selected for satisfactory performance at the location E under no climate perturbations (i.e., no changes in P_{avg} and T_{avg} relative to 1996-2015). Figure 7-6 displays the climatic bounds at which the probability of $\rho_e > 0.70$ (hereafter referred to as π_{e70}) is 95% for all the locations requiring instreamflow. (hereafter referred to as π_{e70}). As expected from Figure 6, the bound for the location E was the highest, and the climate zone for $\pi_{e70} > 95\%$ sensitively declines with rising T_{avg} . The bound for $\pi_{e95} = 95\%$ at the sub-basin 3001 (orange-black dashed line) was below the bounds for the locations E and F. The human-demand-only operations would increase the risks of ecosystem degradation near the locations E and F if climate becomes drier towards drier conditions. The environmental risks at the locations E and F seem to be more sensitive to rising T_{avg} than the water supply risk at the sub-basin 3001. The 50 GCM projections for 2020-2039 predicted that π_{e70} at the location E would drop by 32% relative to 1995-2015. Only 6.5 out of the 50 GCMs for 2020-2039 (12.10%) indicate $\pi_{e70} > 95\%$ at the location E. fell within the range mutually satisfying $\pi_{e95} > 95\%$ and $\pi_{e70} > 95\%$ for every demand node and for the all locations requiring the minimum flows.

4.3 Consideration of ing the instream flow the instreamflow into water management

From the assessments with the logistic response surfaces and the GCM projections, the environmental risk at the location E for 2020-2039 was likely to become an issue for 2020-2039 due to climate change. As an adaptation strategy, the instreamflow flows could be considered in water management to be balanced between water supply and environmental risks. We modelled this scenario this management option by including the environmental instreamflow requirement at the location E in the objective function for of the water allocation model the sequential optimizations as:

$$\text{Minimize } \frac{\sum D_i - \sum S_i}{\sum D_i} - \frac{\sum V_i - \sum C_i}{\sum C_i} + w \frac{Q_{min,E} - Q_E}{Q_{min,E}} \quad (4)$$

where, $Q_{min,E}$ and Q_E are the instream-flow requirement and the streamflow flow at the location E, respectively. w is a weight representing the relative importance of the instreamflow in water management flow deficiency against the environmental requirement. While the minimum instream-flow requirement at the location E could be treated as a constraint for optimizations, this approach may lead to no optimal solutions under severe climate stresses. Hence, it would be better to consider the environmental instreamflow requirement in the objective function for the stress tests varying climate stresses. Through trial and error experiments with the 343-539 climate perturbations, we found that ρ_e at the location E could substantially considerably increase with a small tiny w value. The sequential optimizations with $w=0.01$ allowed us to have a fairly improved ρ_e value at the location E. However, we found that the improved ecological reliability at the location E was by substantial reduction in water supply reliability at the sub-basin 3002. Figure 7 illustrates the logistic models for water supply at the sub-basin 3002 and the instreamflow requirement at the location E under the two operation options applied to

Formatted: Subscript

Formatted: Subscript

Formatted: Not Superscript/ Subscript

Formatted: Not Superscript/ Subscript

the case study. The first operation was only considering the given agricultural and M&I demands (O_1), whereas the deficit against the instreamflow requirement was considered in the second option (O_2). By changing the operation objective from O_1 to O_2 , the risk of $p_c < 0.95$ at the sub-basin substantially increased at the sub-basin 3002. The risk of unsatisfactory water supply was found even with increasing P_{avg} under O_2 . Indeed, the water supply performance became much more sensitive to T_{avg} changes. Conversely, the risk of unsatisfactory ecological reliability at the location E substantially declined. This is because the optimization model did not increase discharge from the sub-basin 3011 for the instreamflow requirement due to the high agricultural demands. Instead, the model forced to increase outflows from the Yongdam dam to meet the agricultural demands at the sub-basins 3012 and 3014 and the instreamflow at the location E. It was inevitable to have deficient water supplies in the sub-basin 3002 with relatively small demands even under optimized water allocations. In other words, minimizing total water deficiency of the entire basin may force the local water deficit in the sub-basin 3002.

4.4 Assessing the management options with the EEDC framework

The two operation options applied in the case study were assessed with the logistic surfaces for the all the sub-basins and the instreamflow locations simultaneously (Figure 8). Table A2 summarizes all the logistic regressions applied in the case study. We simply used the boundaries of $\pi_{s95} = 95\%$ and $\pi_{e70} = 95\%$ for the assessment. With the logistic surfaces, the system robustness to climate change could be measured in the same manner proposed in the original EEDC framework (Poff et al., 2016).

The climate bounds in Figure 8 summarize the two scenarios with and without the environmental requirement. By comparing the middle panels in Figure 8, it is indicated that considering the ~~minimum instreamflow~~ in the objective function significantly lowered the climatic bound of $\pi_{e70} = 95\%$ at the location E, thereby widening the climatic zone within which all the locations mutually satisfy $\pi_{e70} > 95\%$. However, in trade-off, the bound of $\pi_{s95} = 95\%$ for the sub-basin 3002 moved upward, narrowing the climatic zone mutually satisfying $\pi_{s95} > 95\%$ for all the demand nodes. Overall, the climatic zone mutually satisfying $\pi_{s95} > 95\%$ and $\pi_{e70} > 95\%$ for all the ~~sub-basins and instreamflow locations sub-components~~ was expected to decrease when the ~~minimum instream-flow requirement~~ at the location E was considered. Based on ~~the reduced reduction in the mutual climate zone~~, considering the ~~environmental instreamflow requirement in operations would may be unattractive slightly decrease overall system robustness to climate stresses~~ to operators in the Geum River Basin due to the higher priority in human demands.

The decreasing π_{s95} at the sub-basin 3002 could be explained by considering that the instream flow required at the location E should force water retained in the sub-basin 3011 to be released even for low demand seasons. Since the early water release from the sub-basin 3011 should reduce water availability during rice-planting seasons for the sub-basins 3012 and 3014 requiring large agricultural demands, more water resources need be transferred from the dams and the upper sub-basins. Consequently, it was inevitable to have deficient water supplies in the sub-basin 3002 with relatively small demands even

Formatted: Subscript

Formatted: Subscript

Formatted: Subscript

Formatted: Subscript

Formatted: Subscript

Formatted: Subscript

Formatted: Not Superscript/ Subscript

Formatted: Not Superscript/ Subscript

~~under optimized water allocations. In other words, minimizing total water deficiency of the entire basin may force the local water deficit in the sub-basin 3002.~~

~~In summary, The impact assessments using the logistic bounds show that water supply reliabilities at the sub-basins 3001 and 3002 would be the most vulnerable to climate stresses for water supply. The highest environmental risks from climate change would be found at the locations E and F in terms of against the instream-flow requirements. The box plots in Figure 9 display $\pi_{0.95}$ and $\pi_{0.70}$ expected by the 50 GCM collections at the two sub-basins and the two locations. The 50 GCMs projections for 2020-2039 expected almost 100% of $\pi_{0.95}$ at the sub-basins 3002 when the instream flow was not considered. For this extremely low risk in water supply reliability, operators should take a substantial risk of ecosystem degradation in the vicinity of the location E. To reduce the environmental risk at the location E, on the other hand, fairly increasing risks of $p_{\leq 0.95}$ at the sub-basin 3002 should be accepted. Only 4 out of the 50 GCMs indicated $\pi_{0.95} \geq 0.95$.~~

~~The water supply and environmental reliabilities at the sub-basin 3001 and the location F seems to be minimally affected by the minimum flow requirement at the location E.~~

Formatted: Not Superscript/ Subscript

5 Discussion and conclusions

5.1 Use of the ~~The~~ logistic response surfaces for ~~climat change~~ impact assessment of ~~climate change~~

The ~~ordinary~~ response surfaces allowed users to estimate the expected performances of hydrologic systems in response to climate stressors, providing convenience to promptly evaluate many GCM projections (e.g., ~~Steinschneider-Turner et al., 2015a~~2014; Brown et al., 2012; Prudhomme et al., 2010). Nevertheless, ~~the response surface of performance metrics they could might~~ provide insufficient probabilistic information needed for decision-making processes. ~~A possible approach to evaluating the risk of unsatisfactory performances was to count the GCM projections satisfying a pre-defined threshold (e.g., Moursi et al., 2017; Brown et al., 2012). It is possible to count the climate projections satisfying a desired threshold from a collection of GCMs using the ordinary response surface (e.g., Moursi et al., 2017).~~ However, the GCM counts ~~are highly dependent on the size of the GCM collections, do not represent the probability of successive performance, but an expectation of system performance.~~ Even in the case that all the GCMs projections in users' hand fall within the ~~desirable-favourable~~ climate zone ~~on the response surfaces above the threshold, it does not guarantee would not imply~~ that future system performance ~~would will~~ be ~~successive-satisfactory~~ at 100% confidence.

The logistic response surface could supplement the weakness of the ~~ordinary climate~~ response ~~surfaces~~function. It enables to directly ~~evaluate the risk of estimate the probability of successive performance system failures~~ from a single climate projection, ~~allowing users to perceive potential risks of unsatisfactory performance associated with the projection.~~ The probability estimates from the logistic ~~surfaces response function~~ can play a role in risk-based decision-making particularly when an adaptive solution ~~should be is~~ targeted at a particular climate prediction (e.g., resizing infrastructures for a reference

climate condition). The logistic surface developed for the adaptive solution may directly provide the risk of system failures under the climate prediction.

Hence, we attempted to comparatively evaluate the $\pi_{0.95}$ and $\pi_{0.70}$ values from the logistic surfaces using a typical stochastic resampling with the same system models. For the validation, three arbitrary perturbations were selected as (-37.1%, +2.5°C), (-27.7%, +1.3°C), (-13.6%, +0.6°C) for P_{avg} and T_{avg} , respectively. Then, 100 sets of 20-year-long weather series were generated for each perturbation using the stochastic weather generator, and the system models were forced by the generated weather series. By counting the cases satisfying $\rho_s > 0.95$ or $\rho_s > 0.70$ among the 100 simulations, the probability estimates at the sub-basins and instreamflow locations were obtained for each perturbation. Figure 9 shows the 1:1 plot comparing the probability estimates gained from the stochastic sampling and the logistic regressions for the three perturbations. The probability estimates from the two approaches agreed approximately. The stochastic sampling was to quantify the impacts of internal climate variability within a bi-decadal period; however, it may require unacceptable computational costs. 300 sets of stress tests were necessary only for the three perturbations. The 1:1 plot in Figure 9 may imply that the impacts of internal climate variability could be approximately captured by the logistic regression that described collective behaviours of the 539 stress tests. If affordable, a more rigorous validation may be possible with a higher number of stochastic weather generations with additional perturbations.

~~If the ordinary and the logistic responses surfaces together, decision makers can more clearly understand the probability of successive (or non-successive) outcomes together with the expected performance under varying climatic stresses.~~

5.2 Eco-engineering decision scaling with the logistic ~~climate bound~~ surfaces

The ~~EEDC framework eco-engineering decision scaling~~ (Poff et al., 2016) integrates the responsive behaviours of multiple performance metrics into a single climate space. By measuring the size of the climate zone mutually satisfying the multiple criteria, decision-makers can perceive the robustness of system performance with conflicting interests. The decision-makers may select solutions that can widen the mutual climate zone for robust adaptations to climate change. Poff et al. (2016) provided a prominent example that assessed adaptation costs and potential environmental risks with this framework in order to find the most robust strategies in a dam site to climate change. In this study, we showed the advantage of this framework to explore performances at many sub-components of a large system in a single climate domain.

One difference between this study and Poff et al. (2016) is that we used the logistic climate bounds to measure the size of the mutual climate zone satisfying the multiple probabilistic thresholds. ~~Since The—the original EEDC framework eco-engineering decision scaling—was focused on the expected system performances, since the ordinary response surfaces were used. Then,~~ a question can be raised as to “what if no climate projections fall within the mutual climate zone?” In this case, stakeholders may perceive unacceptable risks even though ~~the an~~ adaptive solutions can enlarge the mutual climate zone for multiple criteria. By its nature, the EEDC considering multiple criteria should have a narrower acceptable climate zone than a single-criterion assessment. On the other hand, if If the logistic response surfaces were employed instead, users can estimate the probability of successive outcomes from each climate projection as well as the mutual zone for multiple criteria.

~~The logistic eco-engineering decision-sealing can simultaneously measure show how much system robustness can be obtained from an adaptive solution and how much risks of system non-successive outcomes are indicated by climate projections. Hence, The logistic surfaces may be useful to support for risk-based decision-making processes, the logistic decision-sealing may be more supportive than the original one.~~

5 5.3 Limitations

There are several caveats in ~~this-the case~~ study. First, the monthly operations to balance between water scarcity and storages might be only a part of operators' interests. The stakeholders in practice may have conflicting interests (e.g., reducing flood risks vs. increasing water storage) rather than taking actions toward the single objective. Thus, this study should be deemed a special case focused on the maximum supply reliability under the given operational objectives. A validated simulation model for water allocation will be needed for a more realistic application.

~~Second, the climate bounds of $\pi=95\%$ developed in this study indicate the maximum climatic stresses in which the sub-systems of the river basin can successively perform at 95% confidence. These limits are unnecessarily decision thresholds, but indicators of potential risks. To determine the decision thresholds, the ordinary response surface would be more useful. The logistic response surfaces may be beneficial for risk-based decision-making against pre-defined stakeholder-driven thresholds.~~

~~Finally~~Second, it was unavoidable for us to use many simplifications and assumptions for modelling optimal water managements in the study river basin with complicated features (e.g., monthly dam operations and simple temperature perturbations). Given the substantial uncertainty sources associated with system models in the hydrologic models, the risks of system failures might be greater than our assessments. The logistic surfaces in this work would only consider the impacts of internal climatic variability on system performances.

~~the uncertainty allowance of logistic response surfaces the needs to be evaluated. Expensive efforts may be required for reliable uncertainty analyses.~~

5.4 Conclusions

In this study, we ~~proposed to incorporate the logistic regression into a decision-centric framework for probabilistic impact assessments. The proposed approach requires no more stress tests than typical response-surface-based assessments, albeit some validation is needed. Thus, it may be an efficient method to support risk-based decision making processes. assessed water supply reliability in a river basin with complex features using logistic climate response functions with the eco-engineering decision-sealing framework.~~ Following conclusions are worth emphasizing:

(1) The logistic ~~response surfaces~~ can provide convenience to explore potential risks of ~~system failures unsatisfactory outcomes when against~~ a pre-defined ~~performance~~ threshold is available in response to climatic stresses, while the ~~ordinary~~

response surface can show system performance ~~only~~. On the logistic surfaces, the risk of system failures could be directly indicated by individual GCMs.

(2) Within the ~~The~~ eco-engineering decision scaling framework, the logistic surfaces can be flexibly used to evaluate robustness of hydrological systems to climate stressors. Multi-faceted stakeholders' interests can be considered in a domain of probability performance at sub-components of a complex hydrologic system. By integrating responsive behaviours of all the sub-components into one single climatic space, users can easily find the most vulnerable sub component to climate stressors.

(3) The logistic eco engineering decision scaling may be more supportive than the original framework for risk based decision-making processes in utilizing adaptation strategies. The potential risks of unsuccessful outcomes contained in adaptive solutions can be evaluated from a single climate projection in addition to the mutual climate zones indicating system robustness to climatic changes.

(4) The case study for the Geum River Basin in South Korea provides an assessment that water supply performance for 2020-2039 seems to be sufficient against the water demands projected to 2030. However, the human-demand-only operations would make the eco-systems increasingly vulnerable. To consider the instream-flow requirement in operations for 2020-2039, risks of insufficient water supply should increase at the upper sub-basins with small water demands.

Acknowledgement

This study was supported by the APEC Climate Center. We send special thanks are very thankful for the water demand data provided by the team leading for the national water resources plan at the Korea Institute of Civil Engineering and Building Technology. The GCMs downscaled by Dr. Hyung-II Eum at the Alberta Environment and Parks are greatly appreciated. All authors declare no conflict of interests. The data required to reproduce the results are available upon request from the authors (d.kim@apcc21.org, sjchoi@kict.re.kr).

References

- Allen, R. G., Pereira, L. S., Raes, D., and Smith, M.: Crop Evapotranspiration: Guidelines for Computing Crop Water Requirement, FAO Irrig. Drain., Paper No. 56, Food and Agriculture Organization of the United Nations, Rome, Italy, 1998.
- Apipattanas, S., Podesta, G., Rajagopalan, B., and Katz, R. W.: A semiparametric multivariate and multisite weather generator, *Water Resour. Res.*, 43, W11401, <https://doi.org/10.1029/2006WR005714>, 2007
- Bae, D. H., Jung, I. W., and Chang, H.: Long term trend of precipitation and runoff in Korean river basins, *Hydrol. Process.*, 22, 2644-2656, 2008.
- Barron, E. J.: Beyond climate science, *Science*, 326, 643, 2009.

Brown, C. M., Lund, J. R., Cai, X., Reed, P. M., Zagana, E. A., Ostfeld, A., Hall, J., Characklis, G. W., Yu, W., and Brekke, L.: The future of water resources systems analysis: Toward a scientific framework for sustainable water management, *Water Resour. Res.*, 51, 6110–6124, <https://doi.org/10.1002/2015WR017114>, 2015.

Brown, C., and Wilby, R. L.: An alternate approach to assessing climate risks. *Eos Trans. AGU*, 93(41), 401, 2012.

5 Brown, C., Ghile, Y., Lavery, M., and Li, K.: Decision scaling: linking bottom up vulnerability analysis with climate projections in the water sector. *Water Resour. Res.*, W09537, <https://doi.org/10.1029/2011WR011212>, 2012.

Bürger, G., Sobie, S. R., Cannon, A. J., Werner, A. T., and Murdock, T. Q.: Downscaling extremes: an intercomparison of multiple methods for future climate. *J. Clim.*, 26(10), 3429–3449, <https://doi.org/10.1175/JCLI-D-12-00249.1>, 2013.

Cannon, A. J., Sobie, S. R., and Murdock, T. Q.: Bias correction of GCM precipitation by quantile mapping: How well do methods preserve changes in quantiles and extremes?, *J. Clim.*, 28, 6938–6959, 2015.

10 Perrin, C., Oudin, L., Andreassian, V., Rojas-Serna, C., Michel, C., and Mathevet, T.: Impact of limited streamflow data on the efficiency and the parameters of rainfall runoff models, *Hydrolog. Sci. J.*, 52, 131–151, <https://doi.org/10.1623/hysj.52.1.131>, 2010.

Cosgrove, W. J., and Loucks, D. P.: Water management: Current and future challenges and research directions, *Water Resour. Res.*, 51, 4823–4839, <https://doi.org/10.1002/2014WR016869>, 2015.

15 Culley, S., Noble, S., Yates, A., Timbs, M., Westra, S., Maier, H. R., Giuliani, M., and Castelletti, A.: A bottom-up approach to identifying the maximum operational adaptive capacity of water resource systems to a changing climate, *Water Resour. Res.*, 52, 6751–6768, <https://doi.org/10.1002/2015WR018253>, 2016.

Daly, C., Halbleib, M., Smith, J. I., Gibson, W. P., Doggett, M. K., Taylor, G. H., Curtis, J., and Pasteris, P. P.: Physiographically sensitive mapping of climatological temperature and precipitation across the conterminous United States, *Int. J. Climatol.*, 28, 2031–2064, <https://doi.org/10.1002/joc.1688>, 2008.

20 Demirel, M. C., Booi, M. J., and Hoekstra, A. Y.: The skill of seasonal ensemble low flow forecasts in the Moselle River for three different hydrological models, *Hydrol. Earth Syst. Sci.*, 19, 275–291, <https://doi.org/10.5194/hess-19-275-2015>, 2015.

25 Deser, C., Phillips, A., Bourdette, V., and Teng, H.: Uncertainty in climate change projections: the role of internal variability, *Clim. Dyn.*, 38, 527–546, doi:10.1007/s00382-010-0977-x, 2012.

Doherty, S. J., Bojinski, S., Henderson-Sellers, A., Noone, K., Goodrich, D., Bindoff, N. L., Church, J. A., Hibbard, K. A., Karl, T. R., Kajfez Bogataj, L., Lynch, A. H., Parker, D. E., Prentice, I. C., Ramaswamy, V., Saunders, R. W., Smith, M. S., Steffen, K., Stoecker, T. F., Thorne, P. W., Trenberth, K. E., Verstraete, M. M., and Zwiers, F. W.: Lessons learned from IPCC AR4: Scientific developments needed to understand, predict, and respond to climate change, *Bull. Am. Meteorol. Soc.*, 90, 497–513, 2009.

30 Dufresne, J.-L., and Bony, S.: An assessment of the primary sources of spread of global warming estimates from coupled atmosphere-ocean models, *J. Clim.*, 21, 5135–5144, 2008.

Eum, H. I., and Cannon, A. J.: Interecomparison of projected changes in climate extremes for South Korea: Application of trend-preserving statistical downscaling methods to the CMIP5 ensemble. *Int. J. Climatol.*, 37(8), 3381–3397, 2017.

Eum, H. I., and Simonovic, S. P.: Integrated reservoir management system for adaptation to climate change: The Nakdong River Basin in Korea. *Water Resour. Manage.*, 24, 3397–3417, 2010.

5 Georgakakos, A. P., Yao, H., Kistenmacher, M., Georgakakos, K. P., Graham, N. E., Cheng, F. Y., Spencer, C., and Shamir, E.: Value of adaptive water resources management in Northern California under climatic variability and change. *Reservoir management, J. Hydrol.*, 412–413, 34–46, <https://doi.org/10.1016/j.jhydrol.2011.04.038>, 2012.

Goddard, L., Baethgen, W., Kirtman, B., and Meehl, G.: The urgent need for improved climate models and predictions. *Eos Trans. AGU*, 90(39), 343, 2009.

10 Haasnoot, M., Kwakkel, J. H., Walker, W. E., and ter Maat, J.: Dynamic adaptive policy pathways: A method for crafting robust decisions for a deeply uncertain world. *Glob. Environ. Change*, 23, 485–498, 2013.

Hadka, D., Herman, J., Reed, P., and Keller, K.: An open source framework for many objective robust decision making. *Environ. Model. Softw.*, 74, 114–129, 2015.

Herman, J. D., Zeff, H. B., Reed, P. M., and Charaklis, G. W.: Beyond optimality: Multistakeholder robustness tradeoffs for regional water portfolio planning under deep uncertainty. *Water Resour. Res.*, 50, 7692–7713, <https://doi.org/10.1002/2014WR015338>, 2014.

15 Hwang, S. and Graham, W. D.: Development and comparative evaluation of a stochastic analog method to downscale daily GCM precipitation. *Hydrol. Earth Syst. Sci.*, 17, 4481–4502, <https://doi.org/10.5194/hess-17-4481-2013>, 2013.

IPCC: Climate Change 2007: Synthesis Report. Contribution of Working Groups I, II and III to the Fourth Assessment Report of the Intergovernmental Panel on Climate Change [Core Writing Team, Pachauri, R.K and Reisinger, A.(eds.)]. IPCC, Geneva, Switzerland, 104 pp., 2007.

20 Jowett, I. G.: Instream flow methods: a comparison of approaches. *Regul. Rivers: Res. Mgmt.*, 13, 115–127, 1997.

Jung, Y., and Eum, H. I.: Application of a statistical interpolation method to correct extreme values in high-resolution gridded climate variables. *J. Clim. Chang. Res.*, 6, 331–334, 2015.

25 Kay, A. L., Crooks, S. M., and Reynard, N. S.: Using response surfaces to estimate impacts of climate change on flood peaks: assessment of uncertainty. *Hydrol. Process.*, 28, 5273–5287, <https://doi.org/10.1002/hyp.10000>, 2014.

Kim, D., Jung, I. W., and Chun, J. A.: A comparative assessment of rainfall-runoff modelling against regional flow duration curves for ungauged catchments. *Hydrol. Earth Syst. Sci.*, 21, 5647–5661, <https://doi.org/10.5194/hess-21-5647-2017>, 2017.

30 Kim, D.: A Decision-centric Assessment for Water Resources Management in a Large River Basin under Non-Stationary Climate. APEC Climate Center Research Report 2017-18, 2018.

Korteling, B., Dessai, S., and Kapelan, Z.: Using information gap decision theory for water resources planning under Severe Uncertainty. *Water Resour. Manage.*, 27, 1149–117, <https://doi.org/10.1007/s11269-012-0164-4>, 2013.

- Kwon, H. H., Lall, U., and Khalil, A. F.: Stochastic simulation model for nonstationary time series using an autoregressive wavelet decomposition: Applications to rainfall and temperature, *Water Resour. Res.*, 43, W05407, <https://doi.org/10.1029/2006WR005258>, 2007.
- Lampert, R. J., and Groves, D. G.: Identifying and evaluating robust adaptive policy responses to climate change for water management agencies in the American west, *Technol. Forecasting Soc. Change*, 77, 960-974, 2010.
- Lee, H., Chun, J. A., Han, H. H., and Kim, S.: Prediction of frost occurrences using statistical modeling approaches, *Adv. Meteorol.*, 2075186, <http://doi.org/10.1155/2016/2075186>, 2016.
- Ministry of Construction and Transportation (MOCT): National Water Resources Plan (Water Vision 2020), Daejeon, South Korea, 2000.
- Ministry of Construction and Transportation (MOCT): National Water Resources Plan (2006-2020), Daejeon, South Korea, 2006.
- Ministry of Land, Transport and Maritime Affairs (MLTM): National Water Resources Plan (2011-2020), Daejeon, South Korea, 2011.
- Ministry of Land, Infrastructure and Transport (MOLIT): National Water Resources Plan (2001-2020) — 3rd revision (2016-2020), 2016.
- Moursi, H., Kim, D., and Kaluarachchi, J. J.: A probabilistic assessment of agricultural water scarcity in a semi-arid and snowmelt-dominated river basin under climate change, *Agric. Water Manage.*, 193, 142-152, 2017.
- Oudin, L., Kay, A., Andréassian, V., and Perrin, C.: Are seemingly physically similar catchments truly hydrologically similar?, *Water Resour. Res.*, 46, W11558, <https://doi.org/10.1029/2009WR008887>, 2010.
- Oudin, L., Andréassian, V., Perrin, C., Michel, C., and Le Moine, N.: Spatial proximity, physical similarity, regression and ungauged catchments: a comparison between regionalization approaches based on 913 French catchments, *Water Resour. Res.*, 44, W03413, <https://doi.org/10.1029/2007WR006240>, 2008.
- Perrin, C., Michel, C., and Andréassian, V.: Improvement of a parsimonious model for streamflow simulation, *J. Hydrol.*, 279, 275-289, 2003.
- Piao, S., Ciais P., Huang, Y., Shen, Z., Peng, S., Li, J., Zhou, L., Liu, H., Ma, Y., Ding, Y., Friedlingstein, P., Liu, C., Tan, K., Yu, Y., Zhang, T., and Fang, J.: The impacts of climate change on water resources and agriculture in China, *Nature*, 467, 43-51, 2010.
- Poff, N. L., Brown, C. M., Grantham, T. E., Matthews, J. H., Palmer, M. A., Spence, C. M., Wilby, R. L., Haasnoot, M., Mendoza, G. F., Dominique, K. C., and Baeza, A.: Sustainable water management under future uncertainty with eco-engineering decision making, *Nature Clim. Change*, 6, 25-34, <https://doi.org/10.1038/nclimate2765>, 2016.
- Prudhomme, C., Wilby, R. L., Crooks, S., Kay, A. L., and Reynard, N. S.: Scenario neutral approach to climate change impact studies: Application to flood risk, *J. Hydrol.*, 390, 198-209, <https://doi.org/10.1016/j.jhydrol.2010.06.043>, 2010.
- Rosenberg, D. E.: Blended near-optimal alternative generation, visualization, and interaction for water resources decision making, *Water Resour. Res.*, 51, 2047-2063, <https://doi.org/10.1002/2013WR014667>, 2015.

Schlef, K. E., Steinschneider, S., and Brown, C. M.: Spatiotemporal impacts of climate and demand on water supply in the Apalachicola-Chattahoochee-Flint Basin, *J. Water Resour. Plann. Manage.*, 144, 05017020, 2017.

Shapiro, M., Shukla, J., Brunet, G., Nobre, C., Beland, M., Dole, R., Trenberth, K., Anthes, R., Asrar, G., Barrie, L., Bougeault, P., Brasseur, G., Burridge, D., Busalacchi, A., Caughey, J., Chen, D., Church, J., Enomoto, T., Hoskins, B., Hov, Ø., Laing, A., Le Treut, H., Marotzke, J., McBean, G., Meehl, G., Miller, M., Mills, B., Mitchell, J., Monerieff, M., Nakazawa, T., Olafsson, H., Palmer, T., Parsons, D., Rogers, D., Simmons, A., Troccoli, A., Toth, Z., Uccellini, L., Velden, C., and Wallace, J. M.: An earth system prediction initiative for the twenty first century, *Bull. Am. Meteorol. Soc.*, 91, 1377–1388, 2010.

Stainforth, D. A., Aina, T., Christensen, C., Collins, M., Faull, N., Frame, D. J., Kettleborough, J. A., Knight, S., Martin, A., Murphy, J. M., Piani, C., Sexton, D., Smith, L. A., Spicer, R. A., Thorpe, A. J., and Allen, M. R.: Uncertainty in predictions of the climate response to rising levels of greenhouse gases, *Nature*, 433, 403–406, 2005.

Steinschneider, S., and Brown, C.: A semiparametric multivariate, multisite weather generator with low frequency variability for use in climate risk assessments, *Water Resour. Res.*, 49, 7205–7220, <https://doi.org/10.1002/wrer.20528>, 2013.

Steinschneider, S., and Brown, C.: Dynamic reservoir management with real option risk hedging as a robust adaptation to nonstationary climate, *Water Resour. Res.*, 48, W11525, <https://doi.org/10.1029/2011WR011318>, 2012.

Steinschneider, S., McCrary, R., Wi, S., Mulligan, K., Mearns, L. O., and Brown, C.: Expanded decision scaling framework to select robust long term water system plans under hydroclimatic uncertainties, *J. Water Resour. Plann. Manage.*, 141, 04015023–1, 2015a.

Steinschneider, S., Wi, S., and Brown, C.: The integrated effects of climate and hydrologic uncertainty on future flood risk assessments, *Hydrol. Process.*, 29, 2823–2839, <https://doi.org/10.1002/hyp.10409>, 2015b.

Stevens, B., and Bony, S.: What are climate models missing?, *Science*, 340, 1053–1054, 2013.

Turner, S. W. D., Marlow, D., Ekström, M., Rhodes, B. G., Kularathna, U., and Jeffrey, P. J.: Linking climate projections to performance: A yield-based decision scaling assessment of a large urban water resources system, *Water Resour. Res.*, 50, 3553–3567, <https://doi.org/10.1002/2013WR015156>, 2014.

Vano, J. A., Scott, M. J., Voisin, N., Stöckle, C. O., Hamlet, A. F., Mickelson, K. E. B., Elsner, M. M., and Lettenmaier, D. P.: Climate change impacts on water management and irrigated agriculture in the Yakima River Basin, Washington, USA, *Clim. Change*, 102, 287–317, 2010.

Weaver, C. P., Lempert, R. J., Brown, C., Hall, J. A., Revell, D., and Sarewitz, D.: Improving the contribution of climate model information to decision making: the value and demands of robust decision frameworks, *WIREs Clim. Change*, 4, 39–60, <https://doi.org/10.1002/wcc.202>, 2013.

Whateley, S., Steinschneider, S., and Brown, C.: A climate change range-based method for estimating robustness for water resources supply, *Water Resour. Res.*, 50, 8944–8961, <https://doi.org/10.1002/WR015956>, 2014.

Wilby, R. L., and Dessai, S.: Robust adaptation to climate change, *Weather*, 65, 180–185, <https://doi.org/10.1002/wea.543>, 2010.

Woodward, M., Kapelan, Z. and Gouldby, B.: Adaptive flood risk management under climate change uncertainty using real options and optimization, *Risk Analysis*, 34, 75–92, <https://doi.org/10.1111/risa.12088>, 2014.

Xu, W., Zhao, J., Zhao, T., and Wang, Z.: Adaptive reservoir operation model incorporating nonstationary inflow prediction, *J. Water Resour. Plann. Manage.*, 141, 04014099, 2015.

5 Yan, D., Werners, S. E., Ludwig, F., and Huang, H.Q.: Hydrological response to climate change: the Pearl River, China under different RCP scenarios, *J. Hydrol. Reg. Stud.*, 4, 228–245, 2015.

Zhang, Y., Vaze, J., Chiew, F. H. S., and Li, M.: Comparing flow duration curve and rainfall runoff modelling for predicting daily runoff in ungauged catchments, *J. Hydrol.*, 525, 72–86, 2015.

Zhang, Y., You, Q., Chen, C., and Ge, J.: Impacts of climate change on streamflows under RCP scenarios: A case study in 10 Xin River Basin, China, *Atmos. Res.* 178, 521–534, 2016.

Apipattanavis, S., Podesta, G., Rajagopalan, B., and Katz, R. W.: A semiparametric multivariate and multisite weather generator, *Water Resour. Res.*, 43, W11401, <https://doi.org/10.1029/2006WR005714>, 2007.

Bae, D.-H., Jung, I.-W., and Chang, H.: Long-term trend of precipitation and runoff in Korean river basins, *Hydrol. Process.*, 22, 2644–2656, 2008.

15 Brown, C. M., Lund, J. R., Cai, X., Reed, P. M., Zagona, E. A., Ostfeld, A., Hall, J., Characklis, G. W., Yu, W., and Brekke, L.: The future of water resources systems analysis: Toward a scientific framework for sustainable water management, *Water Resour. Res.*, 51, 6110–6124, <https://doi.org/10.1002/2015WR017114>, 2015.

Brown, C., and Wilby, R. L.: An alternate approach to assessing climate risks. *Eos Trans. AGU*, 93(41), 401, 2012.

Brown, C., Ghile, Y., Laverty, M., and Li, K.: Decision scaling: linking bottom-up vulnerability analysis with climate 20 projections in the water sector. *Water Resour. Res.*, W09537, <https://doi.org/10.1029/2011WR011212>, 2012.

Bürger, G., Sobie, S. R., Cannon, A. J., Werner, A. T., and Murdock, T. Q.: Downscaling extremes: an intercomparison of multiple methods for future climate. *J. Clim.*, 26(10), 3429–3449, <https://doi.org/10.1175/JCLI-D-12-00249.1>, 2013.

Cannon, A. J., Sobie, S. R., and Murdock, T. Q.: Bias correction of GCM precipitation by quantile mapping: How well do methods preserve changes in quantiles and extremes?, *J. Clim.* 28, 6938–6959, 2015.

25 Cosgrove, W. J., and Loucks, D. P.: Water management: Current and future challenges and research directions, *Water Resour. Res.*, 51, 4823–4839, <https://doi.org/10.1002/2014WR016869>, 2015.

Culley, S., Noble, S., Yates, A., Timbs, M., Westra, S., Maier, H. R., Giuliani, M., and Castelletti, A.: A bottom-up approach to identifying the maximum operational adaptive capacity of water resource systems to a changing climate, *Water Resour. Res.*, 52, 6751–6768, <https://doi.org/10.1002/2015WR018253>, 2016.

30 Daly, C., Halbleib, M., Smith, J. I., Gibson, W. P., Doggett, M. K., Taylor, G. H., Curtis, J., and Pasteris, P. P.: Physiographically sensitive mapping of climatological temperature and precipitation across the conterminous United States, *Int. J. Climatol.*, 28, 2031–2064, <https://doi.org/10.1002/joc.1688>, 2008.

Demirel, M. C., Booij, M. J., and Hoekstra, A. Y.: The skill of seasonal ensemble low-flow forecasts in the Moselle River for three different hydrological models, *Hydrol. Earth Syst. Sci.*, 19, 275-291, <https://doi.org/10.5194/hess-19-275-2015>, 2015.

Deser, C., Phillips, A., Bourdette, V., and Teng, H.: Uncertainty in climate change projections: the role of internal variability, *Clim. Dyn.*, 38, 527-546, doi:10.1007/s00382-010-0977-x., 2012.

Dufresne, J.-L., and Bony, S.: An assessment of the primary sources of spread of global warming estimates from coupled atmosphere-ocean models, *J. Clim.*, 21, 5135-5144, 2008.

Eum, H.-I. and Cannon, A. J.: Intercomparison of projected changes in climate extremes for South Korea: Application of trend preserving statistical downscaling methods to the CMIP5 ensemble. *Int. J. Climatol.*, 37(8), 3381-3397, 2017.

Eum, H.-I., and Simonovic, S. P.: Integrated reservoir management system for adaptation to climate change: The Nakdong River Basin in Korea. *Water Resour. Manage.*, 24, 3397-3417, 2010.

Georgakakos, A. P., Yao, H., Kistenmacher, M., Georgakakos, K. P., Graham, N. E., Cheng, F.-Y., Spencer, C., and Shamir, E.: Value of adaptive water resources management in Northern California under climatic variability and change: Reservoir management, *J. Hydrol.*, 412-413, 34-46, <https://doi.org/10.1016/j.jhydrol.2011.04.038>, 2012.

Haasnoot, M., Kwakkel, J. H., Walker, W. E., and ter Maat, J.: Dynamic adaptive policy pathways: A method for crafting robust decisions for a deeply uncertain world, *Glob. Environ. Change*, 23, 485-498, 2013.

Hadka, D., Herman, J., Reed, P., and Keller, K.: An open source framework for many-objective robust decision making, *Environ. Model. Softw.*, 74, 114-129, 2015.

Hwang, S. and Graham, W. D.: Development and comparative evaluation of a stochastic analog method to downscale daily GCM precipitation, *Hydrol. Earth Syst. Sci.*, 17, 4481-4502, <https://doi.org/10.5194/hess-17-4481-2013>, 2013.

Jowett, I. G.: Instream flow methods: a comparison of approaches. *Regul. Rivers: Res. Mgmt.*, 13, 115-127, 1997.

Jung, Y., and Eum, H.-I.: Application of a statistical interpolation method to correct extreme values in high-resolution gridded climate variables, *J. Clim. Chang. Res.*, 6, 331-334, 2015.

Kav, A. L., Crooks, S. M., and Reynard, N. S.: Using response surfaces to estimate impacts of climate change on flood peaks: assessment of uncertainty, *Hydrol. Process.*, 28, 5273-5287, <https://doi.org/10.1002/hyp.10000>, 2014.

Kim, D., Chun, J. A., and Aikins, C. M.: An hourly-scale scenario-neutral flood risk assessment in a mesoscale catchment under climate change, *Hydrol. Process.*, 32, 3416-3430, <https://doi.org/10.1002/hyp.13273>, 2018.

Kim, D., Jung, I. W., and Chun, J. A.: A comparative assessment of rainfall-runoff modelling against regional flow duration curves for ungauged catchments, *Hydrol. Earth Syst. Sci.*, 21, 5647-5661, <https://doi.org/10.5194/hess-21-5647-2017>, 2017.

Korean Meteorological Administration (KMA) Climatological normals of Korea (1981-2010). Publ. 11-1360000-000077-14, Korea Meteorological Administration, 678 pp. [Available online at http://www.kma.go.kr/down/Climatological_2010.pdf], 2011.

Korteling, B., Dessai, S., and Kapelan, Z.: Using information-gap decision theory for water resources planning under Severe Uncertainty, *Water Resour. Manage.*, 27, 1149-117, <https://doi.org/10.1007/s11269-012-0164-4>, 2013.

[Kwon, H.-H., Lall, U., and Khalil, A. F.: Stochastic simulation model for nonstationary time series using an autoregressive wavelet decomposition: Applications to rainfall and temperature, *Water Resour. Res.*, 43, W05407, <https://doi.org/10.1029/2006WR005258>, 2007.](#)

[Lampert, R. J., and Groves, D. G.: Identifying and evaluating robust adaptive policy responses to climate change for water management agencies in the American west, *Technol. Forecasting Soc. Change*, 77, 960-974, 2010.](#)

[Ministry of Construction and Transportation \(MOCT\): National Water Resources Plan \(Water Vision 2020\), Daejeon, South Korea, 2000.](#)

[Ministry of Construction and Transportation \(MOCT\): National Water Resources Plan \(2006-2020\), Daejeon, South Korea, 2006.](#)

[Ministry of Land, Transport and Maritime Affairs \(MLTM\): National Water Resources Plan \(2011-2020\), Daejeon, South Korea, 2011.](#)

[Ministry of Land, Infrastructure and Transport \(MOLIT\): National Water Resources Plan \(2001-2020\) – 3rd revision \(2016-2020\), 2016.](#)

[Moursi, H., Kim, D., and Kaluarachchi, J. J.: A probabilistic assessment of agricultural waer scarcity in a semi-arid and snowmelt-dominated river basin under climate change, *Agric. Water Manage.*, 193, 142-152, 2017.](#)

[Oudin, L., Kay, A., Andréassian, V., and Perrin, C.: Are seemingly physically similar catchments truly hydrologically similar?, *Water Resour. Res.*, 46, W11558, <https://doi.org/10.1029/2009WR008887>, 2010.](#)

[Oudin, L., Andréassian, V., Perrin, C., Michel, C., and Le Moine, N.: Spatial proximity, physical similarity, regression and unged catchments: a comparison between of regionalization approaches based on 913 French catchments, *Water Resour. Res.*, 44, W03413, <https://doi.org/10.1029/2007WR006240>, 2008.](#)

[Perrin, C., Michel, C., and Andréassian, V.: Improvement of a parsimonious model for streamflow simulation, *J. Hydrol.*, 279, 275-289, 2003.](#)

[Perrin, C., Oudin, L., Andreassian, V., Rojas-Serna, C., Michel, C., and Mathevet, T.: Impact of limited streamflow data on the efficiency and the parameters of rainfall-runoff models, *Hydrolog. Sci. J.*, 52, 131-151, <https://doi.org/10.1623/hysj.52.1.131>, 2010.](#)

[Poff, N. L., Brown, C. M., Grantham, T. E., Matthews, J. H., Palmer, M. A., Spence, C. M., Wilby, R. L., Haasnoot, M., Mendoza, G. F., Dominique, K. C., and Baeza, A.: Sustainable water management under future uncertainty with eco-engineering decision making, *Nature Clim. Change*, 6, 25-34, <https://doi.org/10.1038/nclimate2765>, 2016.](#)

[Prudhomme, C., Wilby, R. L., Crooks, S., Kay, A. L., and Reynard, N. S.: Scenario-neutral approach to climate change impact studies: Application to flood risk, *J. Hydrol.*, 390, 198-209, <https://doi.org/10.1016/j.jhydrol.2010.06.043>, 2010.](#)

[Rosenberg, D. E.: Blended near-optimal alternative generation, visualization, and interaction for water resources decision making, *Water Resour. Res.*, 51, 2047–2063, <https://doi.org/10.1002/2013WR014667>, 2015.](#)

[Schlef, K. E., Steinschneider, S., and Brown, C. M.: Spatiotemporal impacts of climate and demand on water supply in the Apalachicola-Chattahoochee-Flint Basin, *J. Water Resour. Plann. Manage.*, 144, 05017020, 2017.](#)

[Stainforth, D. A., Aina, T., Christensen, C., Collins, M., Faull, N., Frame, D. J., Kettleborough, J. A., Knight, S., Martin, A., Murphy, J. M., Piani, C., Sexton, D., Smith, L. A., Spicer, R. A., Thorpe, A. J., and Allen, M.R.: Uncertainty in predictions of the climate response to rising levels of greenhouse gases, *Nature*, 433, 403–406, 2005.](#)

[Steinschneider, S., and Brown, C.: A semiparametric multivariate, multisite weather generator with low-frequency variability for use in climate risk assessments, *Water Resour. Res.*, 49, 7205–7220, <https://doi.org/10.1002/wrcr.20528>, 2013.](#)

[Steinschneider, S., and Brown, C.: Dynamic reservoir management with real-option risk hedging as a robust adaptation to nonstationary climate, *Water Resour. Res.* 48, W11525, <https://doi.org/10.1029/2011WR011318>, 2012.](#)

[Steinschneider, S., McCrary, R., Wi, S., Mulligan, K., Mearns, L. O., and Brown, C.: Expanded decision-scaling framework to select robust long-term water-system plans under hydroclimatic uncertainties, *J. Water Resour. Plann. Manage.*, 141, 04015023-1, 2015a.](#)

[Steinschneider, S., Wi, S., and Brown, C.: The integrated effects of climate and hydrologic uncertainty on future flood risk assessments, *Hydrol. Process.*, 29, 2823–2839, <https://doi.org/10.1002/hyp.10409>, 2015b.](#)

[Stevens, B. and Bonv, S.: What are climate models missing?, *Science*, 340, 1053-1054, 2013.](#)

[Turner, S. W. D., Marlow, D., Ekström, M., Rhodes, B. G., Kularathna, U., and Jeffrey, P. J.: Linking climate projections to performance: A yield-based decision scaling assessment of a large urban water resources system, *Water Resour. Res.*, 50, 3553–3567, <https://doi.org/10.1002/2013WR015156>, 2014.](#)

[Weaver, C. P., Lempert, R. J., Brown, C., Hall, J. A., Revell, D., and Sarewitz, D.: Improving the contribution of climate model information to decision making: the value and demands of robust decision frameworks, *WIREs Clim. Change*, 4: 39–60, <https://doi.org/10.1002/wcc.202>, 2013.](#)

[Whateley, S., and Brown, C.: Assessing the relative effects of emissions, climate means, and variability on large water supply systems, *Geophys. Res. Lett.*, 43, 11329–11338, <https://doi.org/10.1002/2016GL070241>, 2016](#)

[Whateley, S., Steinschneider, S., and Brown, C.: A climate change range-based method for estimating robustness for water resources supply, *Water Resour. Res.* 50, 8944-8961, <https://doi.org/10.1002/WR015956>, 2014.](#)

[Whateley, S., Steinschneider, S., and Brown, C.: Selecting stochastic climate realizations to efficiently explore a wide range of climate risk to water resource systems, *J. Water Resour. Plann. Manage.*, 142, 06016002, 2016.](#)

[Wilby, R. L. and Dessai, S.: Robust adaptation to climate change, *Weather*, 65: 180-185, <https://doi.org/10.1002/wea.543>, 2010.](#)

[Wilks, D.: Multisite generalization of a daily stochastic precipitation generation model, *J. Hydrol.*, 210, 178-191, 1998.](#)

[Woodward, M., Kapelan, Z. and Gouldby, B.: Adaptive flood risk management under climate change uncertainty using real options and optimization, *Risk Analysis*, 34, 75-92, <https://doi.org/10.1111/risa.12088>, 2014.](#)

[Xu, W., Zhao, J., Zhao, T., and Wang, Z.: Adaptive reservoir operation model incorporating nonstationary inflow prediction, *J. Water Resour. Plann. Manage.*, 141, 04014099, 2015.](#)

[Yan, D., Werners, S. E., Ludwig, F., and Huang, H.Q.: Hydrological response to climate change: the Pearl River, China under different RCP scenarios, *J. Hydrol. Reg. Stud.*, 4, 228–245, 2015.](#)

Zhang, Y., Vaze, J., Chiew, F. H. S., and Li, M.: Comparing flow duration curve and rainfall-runoff modelling for predicting daily runoff in ungauged catchments, J. Hydrol., 525, 72-86, 2015

Zhang, Y., You, Q., Chen, C., and Ge, J.: Impacts of climate change on streamflows under RCP scenarios. A case study in Xin River Basin, China, Atmos. Res. 178, 521–534, 2016.

5

Appendix 1. ~~List of Information of the General Circulation Models~~ and summary of the logistic regression collected from the CMIP5 archive.

Table A1. List of the selected GCMs for the impact assessment under the RCP 4.5 and 8.5 scenarios.

No.	Model Name	Resolution (degree)	Producing Institution
1	CMCC-CM	0.750×0.748	Centro Euro-Mediterraneo per I Cambiamenti Climatici
2	CCSM4	1.250×0.942	National Center for Atmospheric Research
3	CESM1-BGC	1.250×0.942	
4	CESM1-CAM5	1.250×0.942	
5	MRI-CGCM3	1.125×1.122	Meteorological Research Institute
6	CNRM-CM5	1.406×1.401	Centre National de Recherches Meteorologiques
7	HadGEM2-AO	1.875×1.250	Met Office Hadley Centre
8	HadGEM2-CC	1.875×1.250	
9	HadGEM2-ES	1.875×1.250	
10	INM-CM4	2.000×1.500	Institute for Numerical Mathematics
11	IPSL-CM5A-MR	2.500×1.268	Institut Pierre-Simon Laplace
12	MPI-ESM-LR	1.875×1.865	
13	MPI-ESM-MR	1.875×1.865	
14	FGOALS-s2	2.813×1.659	LASG, Institute of Atmospheric Physics, Chinese Academy of Sciences
15	NorESM1-M	2.500×1.895	Norwegian Climate Centre
16	GFDL-ESM2G	2.500×2.023	Geophysical Fluid Dynamics Laboratory
17	GFDL-ESM2M	2.500×2.023	
18	BCC-CSM1-1	2.813×2.791	Beijing Climate Center, China Meteorological Administration
19	BCC-CSM1-1-M	1.125×1.122	
20	IPSL-CM5A-LR	3.750×1.895	Institut Pierre-Simon Laplace
21	IPSL-CM5B-LR	3.750×1.895	
22	MIROC5	1.406×1.401	Atmosphere and Ocean Research Institute, National Institute for Environmental Studies, and Japan Agency for Marine-Earth Science and Technology
23	MIROC-ESM-CHEM	2.813×2.791	
24	MIROC-ESM	2.813×2.791	
25	CanESM2	2.813×2.791	Canadian Centre for Climate Modelling and Analysis

Table A2. The summary of the logistic regressions. The explanatory variables were statistically significant (p-values < 10⁻³) for the all regression models. R² is the McFadden pseudo R².

		O ₁ : Human-demand-only operation				O ₂ : Considering the instreamflow at E			
		Regression coefficients			R ²	Regression coefficients			R ²
		Intersect	ΔP_{ave} (%)	ΔT_{ave} (°C)		Intersect	ΔP_{ave} (%)	ΔT_{ave} (°C)	
<u>Sub-basin</u>	<u>3001</u>	<u>4.38</u>	<u>0.245</u>	<u>-0.630</u>	<u>0.825</u>	<u>3.55</u>	<u>0.234</u>	<u>-0.529</u>	<u>0.813</u>
	<u>3002</u>	<u>14.5</u>	<u>0.401</u>	<u>-0.900</u>	<u>0.878</u>	<u>1.86</u>	<u>0.189</u>	<u>-0.883</u>	<u>0.752</u>
	<u>3003</u>	<u>12.8</u>	<u>0.368</u>	<u>-0.776</u>	<u>0.869</u>	<u>10.3</u>	<u>0.312</u>	<u>-0.605</u>	<u>0.850</u>
	<u>3004</u>	<u>14.1</u>	<u>0.388</u>	<u>-0.872</u>	<u>0.873</u>	<u>13.2</u>	<u>0.363</u>	<u>-0.760</u>	<u>0.865</u>
	<u>3005</u>	<u>12.3</u>	<u>0.405</u>	<u>-0.724</u>	<u>0.887</u>	<u>12.9</u>	<u>0.426</u>	<u>-0.806</u>	<u>0.892</u>
	<u>3006</u>	<u>16.8</u>	<u>0.430</u>	<u>-0.922</u>	<u>0.879</u>	<u>13.6</u>	<u>0.354</u>	<u>-0.812</u>	<u>0.858</u>
	<u>3007</u>	<u>8.97</u>	<u>0.338</u>	<u>-0.866</u>	<u>0.874</u>	<u>7.42</u>	<u>0.295</u>	<u>-0.812</u>	<u>0.858</u>
	<u>3008</u>	<u>21.0</u>	<u>0.528</u>	<u>-1.03</u>	<u>0.898</u>	<u>18.2</u>	<u>0.465</u>	<u>-0.954</u>	<u>0.887</u>
	<u>3009</u>	<u>10.3</u>	<u>0.302</u>	<u>-0.527</u>	<u>0.842</u>	<u>10.3</u>	<u>0.302</u>	<u>-0.527</u>	<u>0.842</u>
	<u>3010</u>	<u>23.6</u>	<u>0.507</u>	<u>-0.654</u>	<u>0.894</u>	<u>22.5</u>	<u>0.470</u>	<u>-0.761</u>	<u>0.883</u>
	<u>3011</u>	<u>11.2</u>	<u>0.383</u>	<u>-0.736</u>	<u>0.882</u>	<u>11.9</u>	<u>0.410</u>	<u>-0.765</u>	<u>0.889</u>
	<u>3012</u>	<u>24.0</u>	<u>0.493</u>	<u>-0.825</u>	<u>0.885</u>	<u>22.5</u>	<u>0.458</u>	<u>-0.790</u>	<u>0.875</u>
	<u>3013</u>	<u>11.4</u>	<u>0.292</u>	<u>-0.396</u>	<u>0.826</u>	<u>11.0</u>	<u>0.284</u>	<u>-0.384</u>	<u>0.821</u>
	<u>3014</u>	<u>21.2</u>	<u>0.439</u>	<u>-0.690</u>	<u>0.871</u>	<u>21.9</u>	<u>0.448</u>	<u>-0.729</u>	<u>0.872</u>
<u>Instreamflow locations</u>	<u>A</u>	<u>28.1</u>	<u>0.644</u>	<u>-1.69</u>	<u>0.920</u>	<u>27.6</u>	<u>0.634</u>	<u>-1.67</u>	<u>0.919</u>
	<u>B</u>	<u>11.1</u>	<u>0.432</u>	<u>-1.11</u>	<u>0.904</u>	<u>10.7</u>	<u>0.423</u>	<u>-1.00</u>	<u>0.902</u>
	<u>C</u>	<u>6.43</u>	<u>0.370</u>	<u>-1.25</u>	<u>0.882</u>	<u>6.51</u>	<u>0.399</u>	<u>-1.31</u>	<u>0.889</u>
	<u>D</u>	<u>25.9</u>	<u>0.445</u>	<u>-0.638</u>	<u>0.800</u>	<u>21.1</u>	<u>0.402</u>	<u>-0.49</u>	<u>0.827</u>
	<u>E</u>	<u>1.47</u>	<u>0.282</u>	<u>-1.08</u>	<u>0.823</u>	<u>7.02</u>	<u>0.533</u>	<u>-1.51</u>	<u>0.912</u>
	<u>F</u>	<u>5.44</u>	<u>0.332</u>	<u>-1.12</u>	<u>0.868</u>	<u>6.52</u>	<u>0.385</u>	<u>-1.32</u>	<u>0.886</u>
	<u>G</u>	<u>14.1</u>	<u>0.591</u>	<u>-1.58</u>	<u>0.934</u>	<u>13.0</u>	<u>0.547</u>	<u>-1.38</u>	<u>0.929</u>

Formatted Table

Table 1: Annual agricultural and M&I demands per demand node and the minimum instream flows from the sub-basins corresponding to the seven locations.

ID No.	Mean annual flow (Mm ³ yr ⁻¹)	Agricultural demand (Mm ³ yr ⁻¹)	M&I demand (Mm ³ yr ⁻¹)	Total storage capacity (Mm ³)	Instream flow requirement (Mm ³ month ⁻¹)	
3001	639.6	50.9	7.6	29.7		
3002	97.3	4.0	0.4	1.0		
3003	254.5	13.1	2.4	5.0		
3004	498.6	50.5	15.8	10.1	8.9 (A)	
3005	382.8	42.3	5.1	14.9	6.6 (B)	
3006	82.6	9.2	3.3	6.8		
Sub-basin node	3007	384.0	74.2	6.1	22.0	7.4 (C)
	3008	473.6	36.9	34.4	7.2	
	3009	465.8	31.5	208.5	7.0	6.7 (D)
	3010	92.2	19.3	16.4	0.2	20.8 (E)
	3011	1145.0	356.6	296.2	100.9	
	3012	1437.2	367.9	75.1	38.4	45.9 (F)
	3013	506.1	193.2	26.4	47.4	6.4 (G)
	3014	340.7	215.1	10.3	29.6	
Outside demand node	OD 1		20.6			
	OD 2		42.1			
	OD 3		5.1			
	OD 4		4.0			
Total	6,800.0	1464.7	779.8	320.2		

* Natural runoff averaged over 20-year rainfall-runoff simulations with stochastic weather series containing zero climatic perturbations ($\Delta P_{\text{avg}} = 0\%$, $\Delta P_{\text{cv}} = 0\%$, $\Delta T_{\text{avg}} = 0\%$) relative to 1996-2015.

I

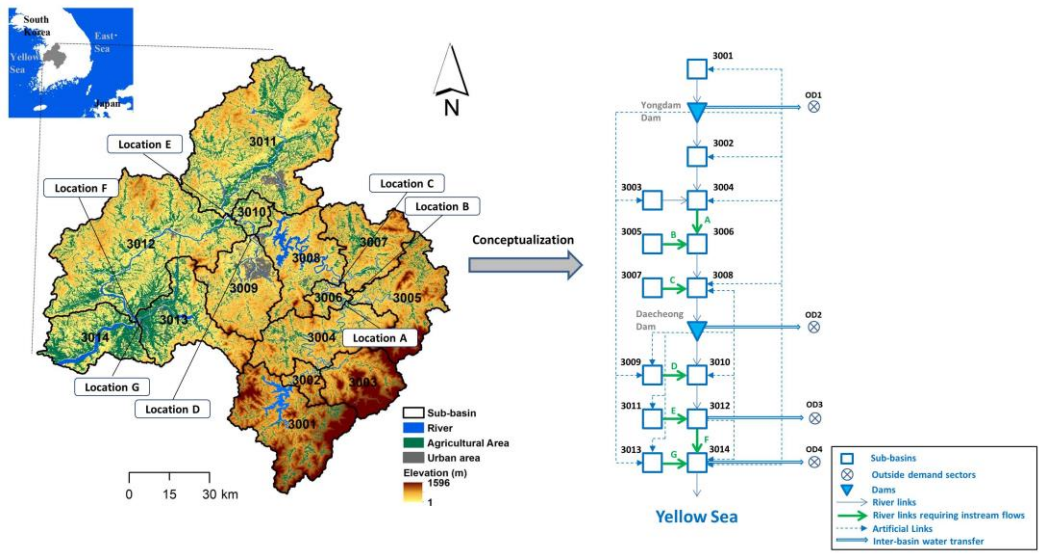


Figure 12: Layout of the Geum River Basins (left) and the simplified node-and-link network for modelling water allocations (right).

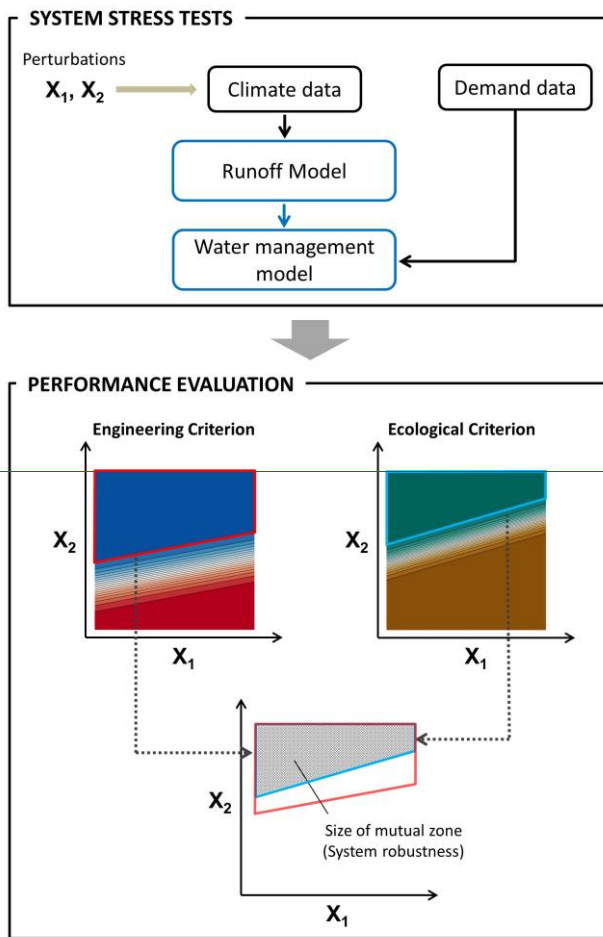


Figure 2: The schematic of the logistic eco-decision scaling framework for evaluating climate change risks with multiple performance criteria.

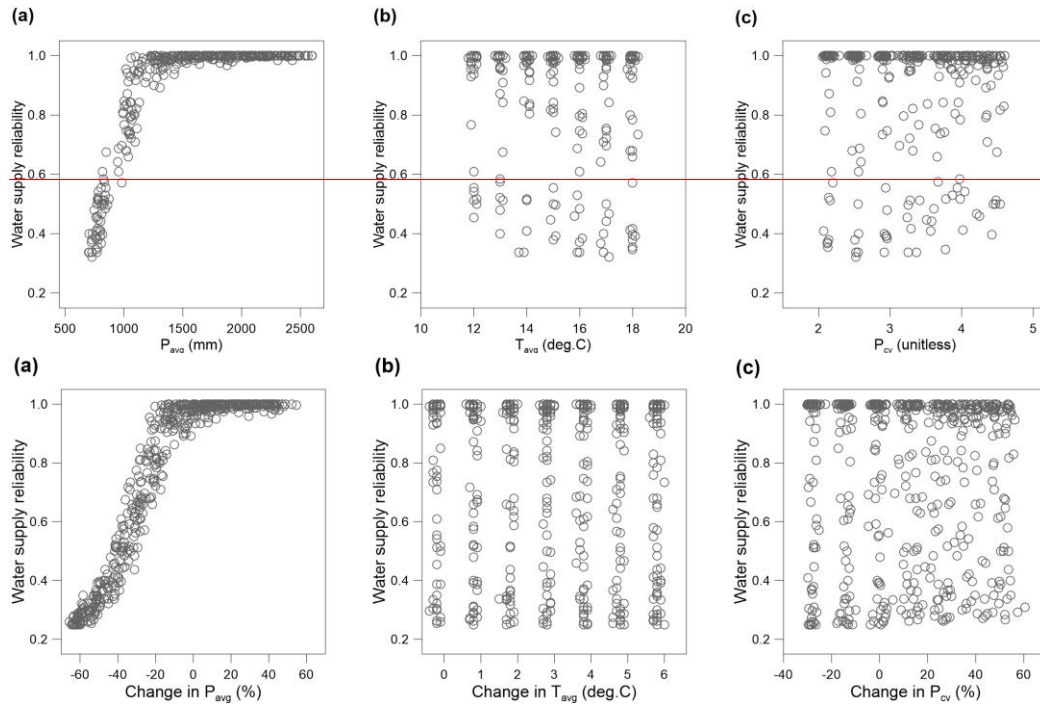
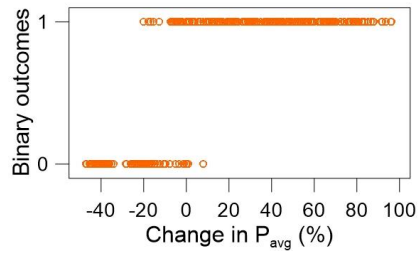
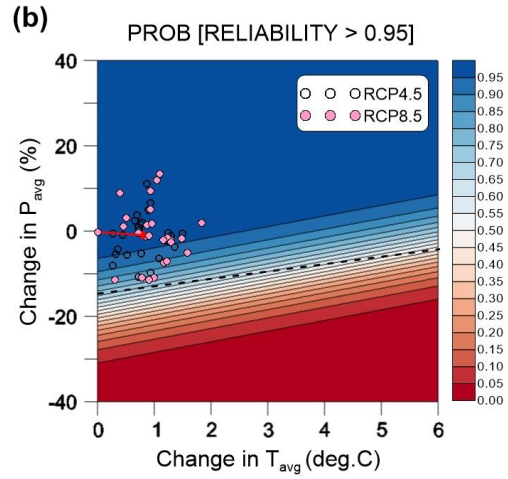
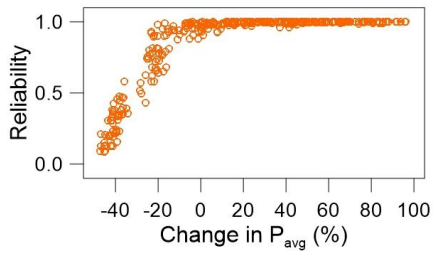
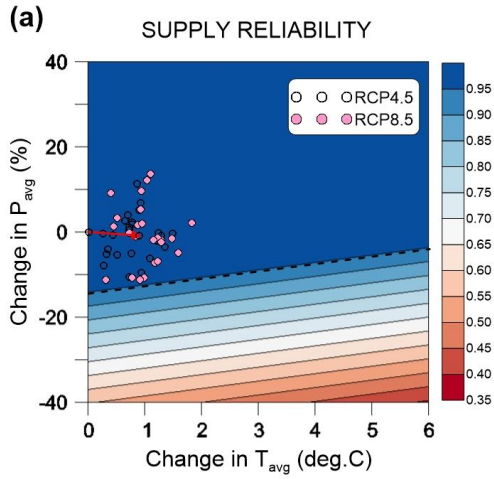


Figure 32: Scatter plots between the water supply reliability samples for at the sub-basin 3001 and changes corresponding in (a) P_{avg} , (b) T_{avg} , and (c) P_{cv} collected from the stress tests with the driven by the 343-539 sets of the stochastically generated stress-imposed weather series.



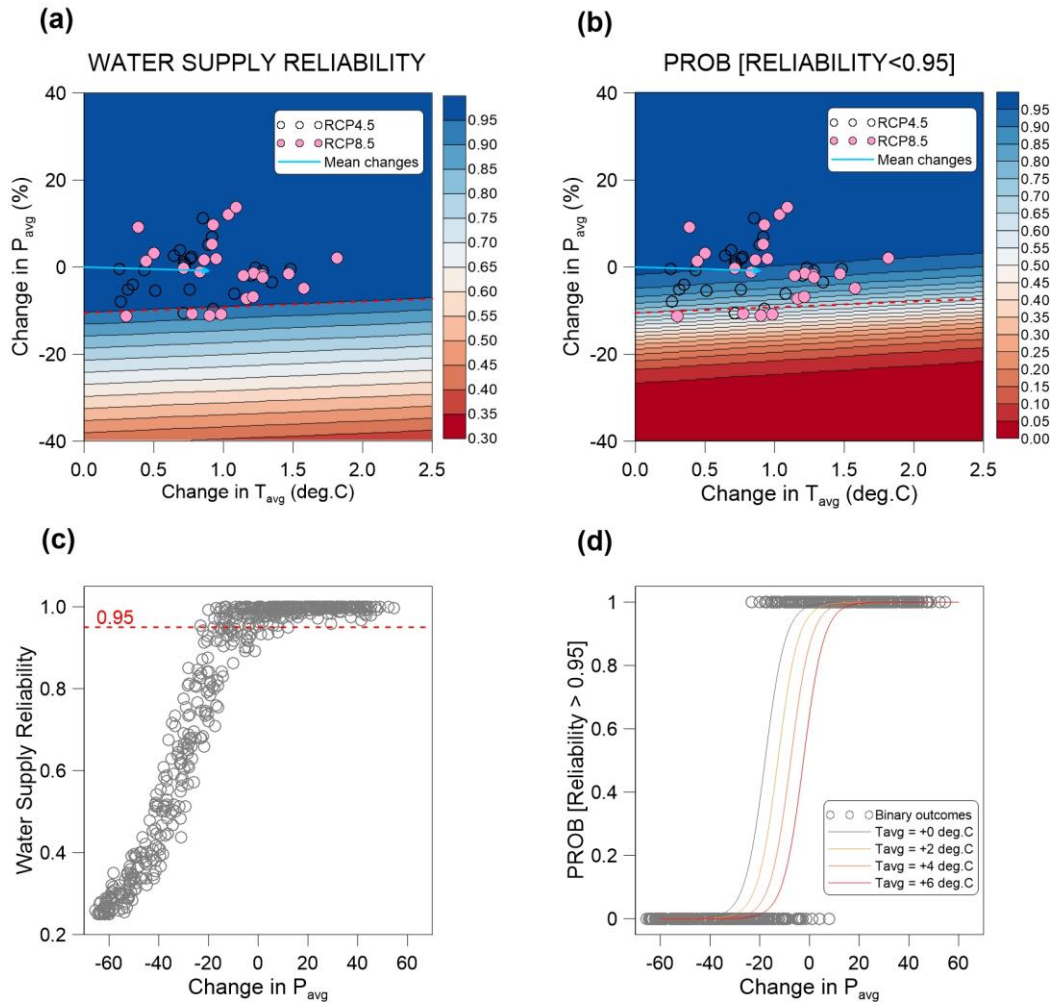


Figure 43: (a) Response surface of ρ_s at the sub-basin 3011 to changes in P_{avg} and T_{avg} , (b) logistic response surface of the probability of $\rho_s > 0.95$ of probability that ρ_s is greater than 0.95, (c) the scatter plot between ρ_s and change in P_{avg} , (d) the binary outcomes against the threshold of $\rho_s > 0.95$ and the sigmoid functions for the probability of $\rho_s > 0.95$. The empty and filled circles overlaid on (a) and (b) are the 50 GCM projections for 2020-2039. The dashed lines in (a) and (b) are the climatic bounds for the climatic threshold of $\rho_s = 0.95$ above which the expected ρ_s would be greater than 0.95.

Formatted: Left

Formatted: Not Superscript/ Subscript

Formatted: Subscript

The bottom panels are the scatter plots between P_{avg} changes and supply reliability (left) and binary outcomes (right) used for the response surfaces, respectively. The changes in P_{avg} and T_{avg} are relative to observed climatology for 1996-2015.

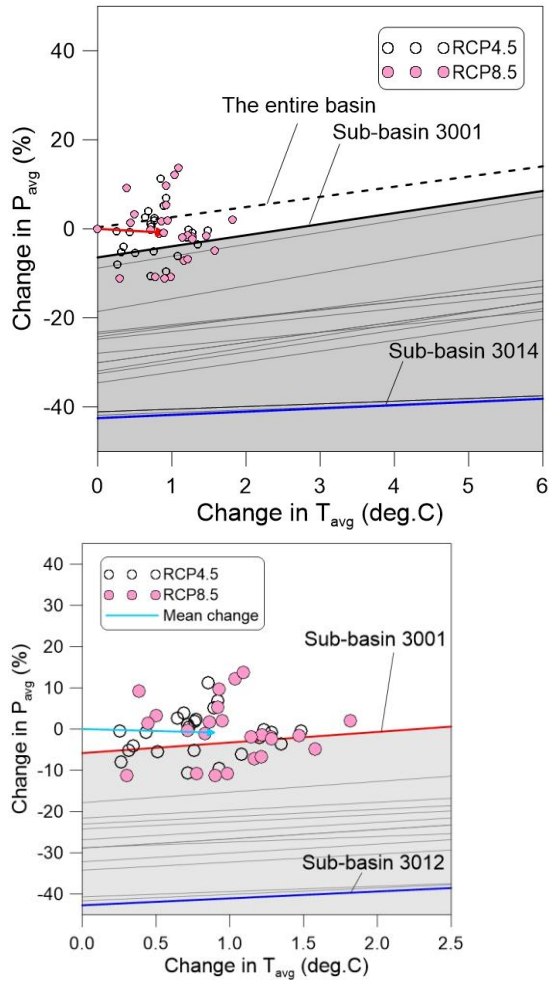


Figure 54: Climatic bounds for $\text{Prob}[p_c > 0.95] = 95\%$, $\pi_{p,90} = 95\%$ for the 14 sub-basins each demand node and the entire basin, on which the 50 GCM projections for 2020-2039 were superimposed. The symbols are the 50 GCMs projections, and the red arrow indicates climatic change to the ensemble of the GCMs for 2020-2039.

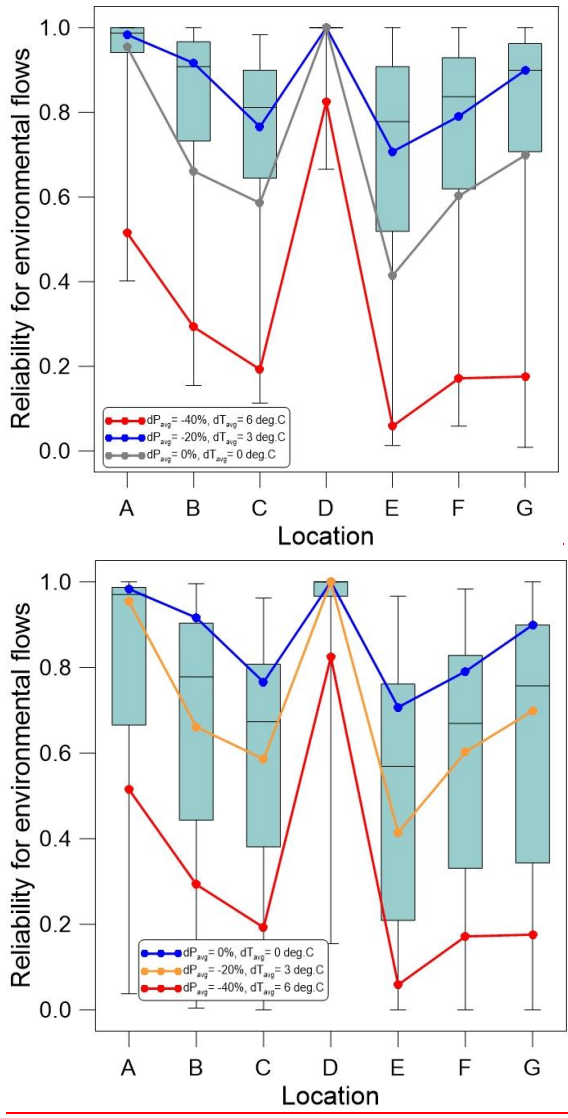
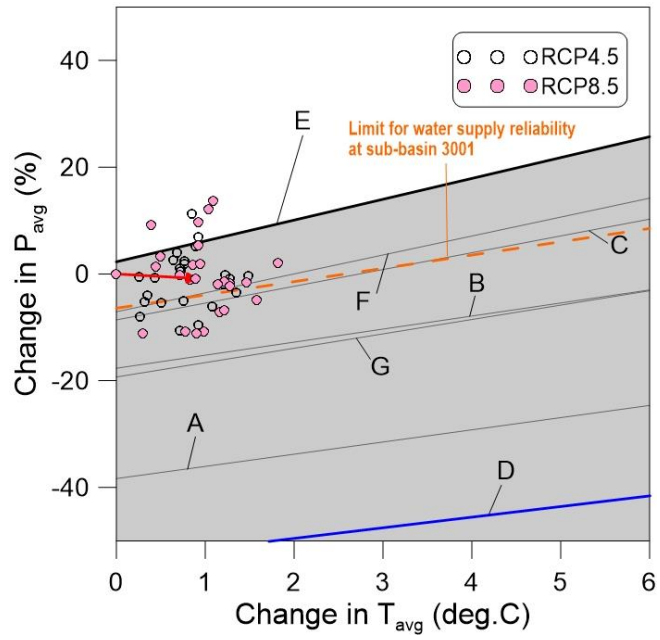


Figure 65: Reliability against the instream flow requirements at the seven locations obtained from the 343-539 sequential optimizations with stress-induced weather series. The blue, grey, and red lines connect the reliabilities at the seven locations under the three representative climatic stresses.

5



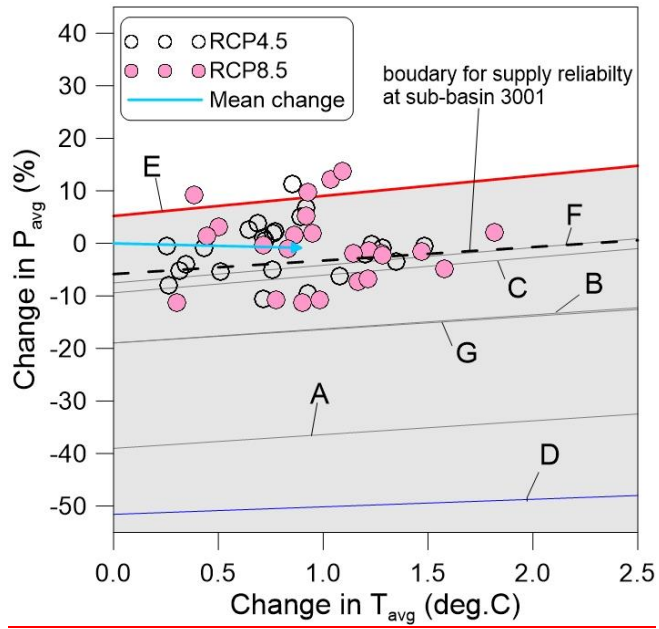


Figure 76: As in Figure 54, but for the probability of $\rho_c > 0.70$ $\pi_{\epsilon_70} = 95\%$ at the seven locations of instreamflow requiring the instream flows for ecosystem sustainability.

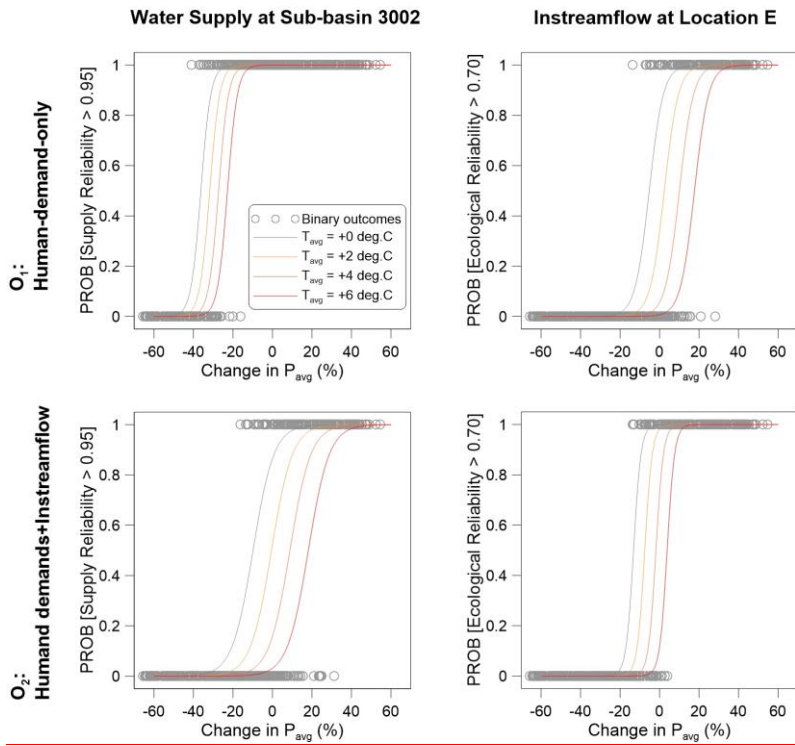


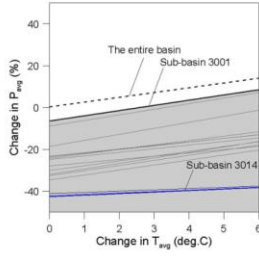
Figure 7: The logistic regression models for $\pi_{0.95}$ at the sub-basin 3002 (left) and $\pi_{0.70}$ at the location E (right) under the human-demand-only operation (upper) and the operation considering human demands and instreamflow together (lower)

Formatted: Caption

Formatted: Not Superscript/ Subscript

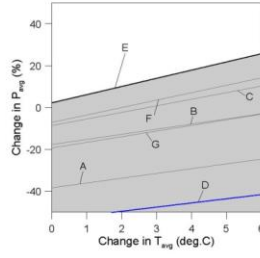
Human demands only

PROB [$\rho_s > 0.95$] = 95%



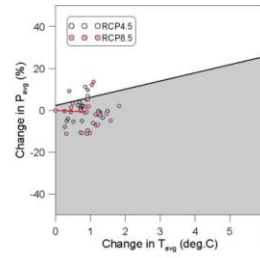
+

PROB [$\rho_e > 0.70$] = 95%

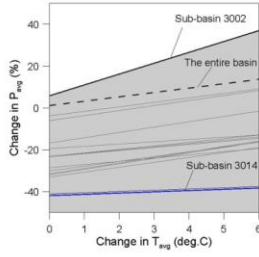


=

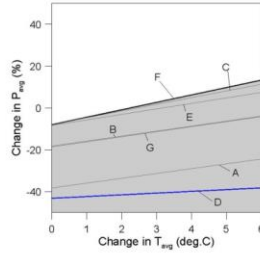
Mutual Bound



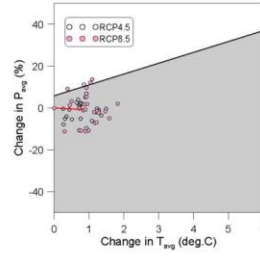
Human demands +
Environmental flows



+



=



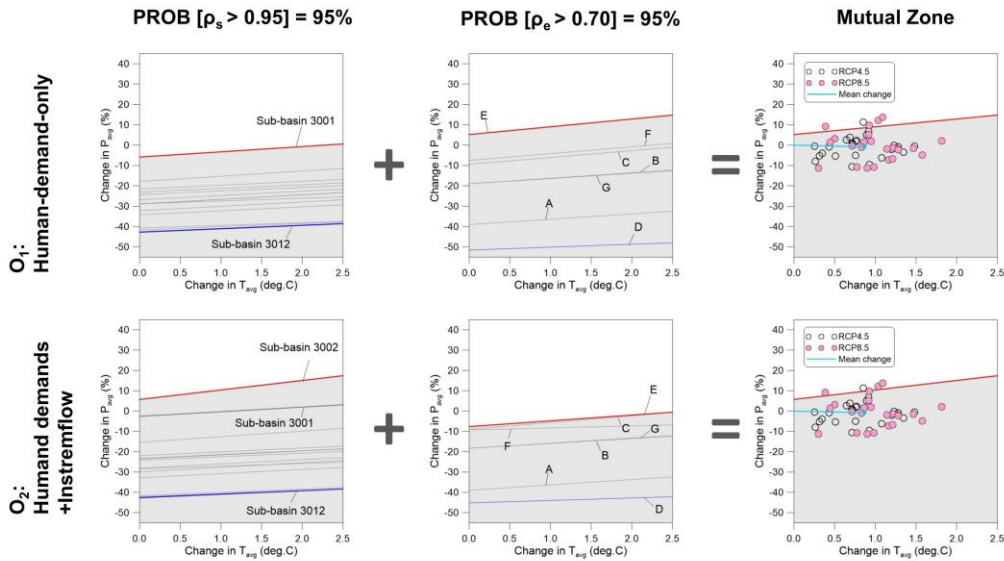


Figure 88: Climatic bounds for $\pi_{0.95} = 95\%$ (left) and $\pi_{0.70} = 95\%$ (middle), and the bound mutually satisfying both criteria (right) under the human-demands-only operations (top) in comparison to the operations considering the instream flows at the location E (bottom). The empty and filled circles are the 50 GCM projections for 2020-2039. The symbols on the right panels are the 50 GCM projections and the arrows indicate climate change to the ensemble of the GCMs for 2020-2039.

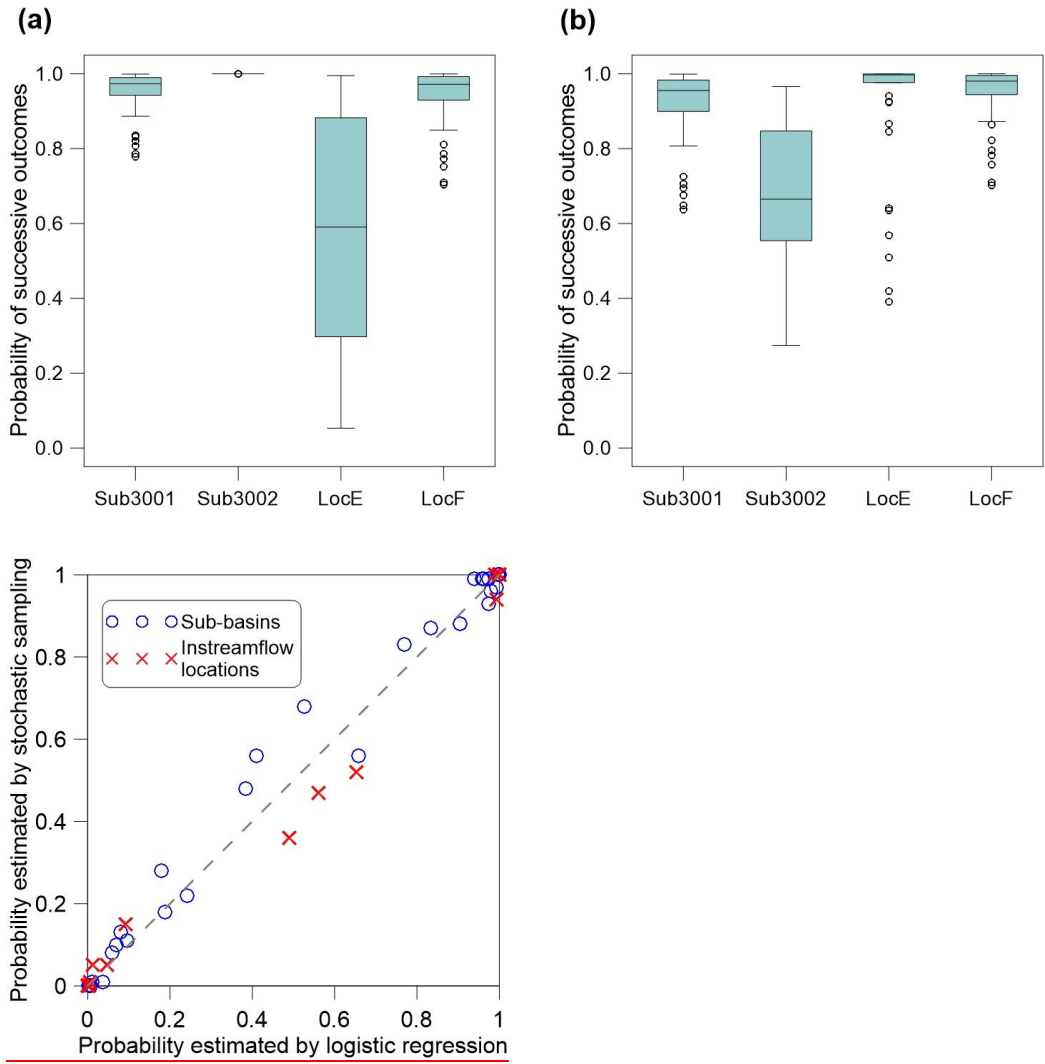


Figure 9: 1:1 plots between the probability estimates from the stochastic sampling and those from the logistic regressions for the case study. Box-plots of $\pi_{0.5}$ and $\pi_{0.25}$ estimated from the 50 GCM projections for 2020-2039 (a) with the human-demands-only operations and (b) with the operations considering the instream-flow requirement at the location E.